表 13　タモキシフェン誘導体処理により肝臓において共通して発現変化の見られた遺伝子

control		Tre	Tam	4OH	ΔC2H5	Tre	Tam	4OH	ΔC2H5	
4h	24h	4h				24h				Gene Name

	FlRaw	F Raw	ratio	FlRaw	ratio	F Raw	ratio	F Raw	ratio	FlRaw	ratio	F Raw	ratio	FlRaw	ratio	F Raw	ratio	F Raw	score	Description
A	65	A	68	3.10	P	207	2.40	P	168	3.05	P	200	4.75	P	321	6.37	P	336	4.45	P	279	6.56	P	414	1.01	A	64	7	growth differentiation factor 15
P	44	P	20	1.94	P	38	6.80	P	139	2.75	P	53	2.35	P	46	18.17	P	759	21.03	P	880	9.80	P	399	1.34	P	57	6	monocyte to macrophage differentiation-as
P	108	P	177	1.55	P	270	1.11	P	203	1.37	P	305	1.53	P	271	4.08	P	422	2.71	P	280	4.63	P	480	2.05	P	216	5	RIKEN cDNA 5730592L21 gene
P	90	P	26	2.52	P	65	3.57	P	98	3.16	P	80	4.76	P	124	1.78	P	152	1.93	P	166	1.73	P	149	1.11	P	96	5	RIKEN cDNA 1700012B18 gene
P	175	P	152	1.57	P	235	1.82	P	288	1.12	P	166	1.81	P	275	2.84	P	477	2.13	P	358	2.52	P	595	1.10	P	186	5	RIKEN cDNA A230075M04 gene
A	31	A	8	7.42	M	61	11.38	P	98	13.17	P	91	7.59	M	63	4.13	P	122	4.96	P	146	3.78	P	111	1.23	A	37	5	interleukin 17 receptor
P	83	P	66	1.83	P	119	1.66	P	113	1.92	P	123	1.77	P	116	1.82	P	145	1.82	P	154	1.97	P	157	1.42	P	114	5	RIKEN cDNA 2010011I20 gene
A	40	A	32	2.00	P	63	1.95	P	64	1.95	P	81	1.56	A	50	2.21	P	84	1.87	P	75	2.40	P	91	1.37	P	52	5	transcription factor 21
P	48	P	89	1.02	P	100	0.78	P	80	0.76	P	74	0.63	P	63	2.83	P	124	2.06	P	95	2.48	P	162	3.82	P	182	4	tubulin, beta 2
P	174	P	250	0.89	P	220	0.89	P	229	0.86	P	209	0.72	P	180	2.00	P	334	2.11	P	352	2.00	P	336	1.88	P	333	4	RIKEN cDNA 2310003F16 gene
A	5	P	48	0.80	P	38	0.59	A	29	0.79	P	37	0.88	A	42	1.61	P	38	6.36	P	42	2.19	P	41	6.91	P	35	4	ubiquitin-conjugating enzyme E2G 2
P	296	P	309	1.42	P	433	1.03	P	329	1.08	P	325	0.98	P	304	1.97	P	531	1.98	P	561	1.86	P	526	1.89	P	484	4	RIKEN cDNA 5730406I15 gene
P	88	P	149	0.97	P	143	1.03	P	159	1.07	P	155	0.89	P	132	4.46	P	376	3.82	P	322	3.07	P	429	2.21	P	188	4	stromal cell-derived factor 2-like 1
P	355	P	754	1.11	P	828	1.13	P	884	1.16	P	857	0.96	P	726	1.89	P	643	1.85	P	629	2.01	P	688	2.32	P	798	4	B-cell receptor-associated protein 37
P	363	P	490	1.35	P	655	0.80	P	403	1.37	P	654	1.10	P	537	2.82	P	910	2.32	P	809	3.26	P	1139	2.18	P	767	4	arginine-rich, mutated in early stage tumor
P	80	P	88	1.18	P	101	1.02	P	93	1.26	P	109	1.11	P	98	2.28	P	131	1.83	P	111	2.61	P	150	1.44	P	142	4	RIKEN cDNA 1200002G13 gene
P	53	M	119	0.82	P	96	0.94	P	116	1.37	P	160	1.12	P	133	2.00	P	101	2.20	P	111	2.11	P	107	2.18	P	111	4	hemopoietic cell phosphatase
P	707	P	595	1.81	P	1062	1.55	P	955	1.51	P	878	1.33	P	792	1.26	P	851	1.81	P	1230	2.04	P	1392	1.72	P	1177	4	RIKEN cDNA 2310020H20 gene
P	654	P	596	1.46	P	863	1.06	P	651	1.04	P	605	1.68	P	987	2.74	P	1716	2.84	P	1843	2.87	P	1618	1.65	P	1042	4	leukemia inhibitory factor receptor
P	96	P	102	1.60	P	161	1.70	P	178	1.87	P	196	1.87	P	190	1.23	P	113	1.14	P	106	1.93	P	176	0.70	P	68	4	inhibin beta E
P	804	P	530	1.68	P	986	1.90	P	1040	1.93	P	996	1.87	P	888	0.92	P	713	0.44	P	342	0.72	P	558	1.15	P	893	4	RIKEN cDNA 3300001H21 gene
P	131	P	32	2.60	P	113	2.60	P	92	2.20	P	88	2.30	P	73	0.68	P	85	0.48	P	61	0.86	P	108	0.96	P	123	4	RIKEN cDNA 2310066P17 gene
A	15	A	7	2.53	A	17	2.46	P	17	2.85	P	24	2.33	A	15	2.59	P	37	3.02	P	44	1.57	M	23	1.76	M	26	4	Mus musculus adult male hypothalamus cD
P	193	P	246	1.69	P	410	1.36	P	345	2.20	P	1773	1.09	P	269	1.54	P	284	2.84	P	545	2.27	P	423	0.85	P	159	4	serum amyloid A 1
A	96	A	13	4.20	A	53	15.06	P	198	7.99	A	99	7.17	A	91	9.72	P	897	12.43	P	1165	8.31	P	582	0.78	A	71	4	monocyte to macrophage differentiation-as

UP-regulated

	FlRaw	F Raw	ratio	FlRaw	ratio	F Raw	ratio	F Raw	ratio	FlRaw	ratio	F Raw	ratio	FlRaw	ratio	F Raw	ratio	FlRaw	ratio	F Raw	score	Description
P	97	P	264	0.51	P	132	0.89	P	188	0.49	P	126	0.38	P	101	0.43	P	40	0.68	P	63	0.36	P	34	1.05	P	99	5	RIKEN cDNA 5830413E08 gene
P	121	P	148	0.48	P	71	0.79	P	120	0.32	P	46	0.87	P	127	0.86	P	100	0.51	P	58	0.40	P	47	0.46	P	54	5	inactive X specific transcripts
P	68	P	84	0.77	P	84	1.03	P	89	0.54	P	44	0.82	P	69	0.43	P	28	0.35	A	23	0.29	A	19	0.53	P	35	5	Mus musculus, clone IMAGE:5068857
P	731	P	1403	0.55	P	768	0.56	P	844	0.72	P	981	0.43	P	598	0.68	P	477	1.10	P	769	0.45	P	313	0.59	P	419	5	lipin 1
P	605	P	240	1.89	P	401	0.71	P	176	1.24	P	291	1.91	P	457	0.40	P	232	0.30	P	174	0.63	P	364	0.50	P	290	4	similar to Isopentenyl-diphosphate delta-is
P	635	P	210	0.96	P	199	1.73	P	374	1.02	P	210	1.19	P	250	0.48	P	295	0.56	P	344	0.50	P	302	0.36	P	219	4	non-POU-domain-containing, octamer bind
P	276	P	110	1.35	P	148	0.87	P	100	1.14	P	123	1.70	P	191	0.48	P	128	0.35	P	92	0.51	P	134	0.58	P	150	4	cytochrome P450, 51
P	192	P	56	1.81	P	100	1.27	P	73	1.15	P	63	1.83	P	102	0.31	P	58	0.40	P	73	0.38	P	70	0.48	P	90	4	retinol dehydrogenase 11
P	139	P	86	1.02	P	87	1.23	P	84	2.17	P	140	1.25	P	83	0.35	P	47	0.33	P	44	0.40	P	53	0.52	P	70	4	bile acid-Coenzyme A: amino acid N-acyltr
P	876	P	1736	0.51	P	868	0.44	P	791	0.57	P	974	0.51	P	890	1.12	P	949	0.90	P	757	1.16	P	971	1.11	P	940	4	DNA segment, Chr 18, ERATO Doi 240, exp
P	237	P	509	0.63	P	317	0.66	P	345	0.53	P	264	0.45	P	229	0.82	P	141	0.71	P	182	0.48	P	109	1.38	P	316	4	glucocorticoid-induced leucine zipper
P	170	P	340	0.35	P	119	0.53	P	187	0.54	P	181	0.29	P	100	0.67	P	110	0.68	P	111	0.70	P	114	0.94	P	154	4	dual specificity phosphatase 1
P	283	P	275	0.47	P	128	0.96	P	272	0.51	P	137	0.55	P	151	0.73	P	199	0.80	P	218	0.39	P	106	0.75	P	205	4	hypothetical protein MGC7221
P	146	P	189	0.57	P	107	0.62	P	122	0.57	P	106	0.57	P	109	0.72	P	102	0.72	P	101	0.52	P	73	0.83	P	117	4	potassium channel, subfamily K, member 5
P	123	P	151	0.60	P	90	0.84	P	131	0.53	A	78	0.62	P	93	0.34	A	40	0.51	A	60	0.57	M	68	0.99	P	118	4	RIKEN cDNA 1110036H21 gene
P	52	P	41	0.60	P	24	1.62	P	69	0.59	M	24	0.99	P	40	0.50	P	25	0.51	P	25	0.29	P	14	0.43	P	21	4	receptor (calcitonin) activity modifying prot
P	832	P	676	0.56	P	371	0.87	P	608	0.77	P	509	0.42	P	285	1.06	P	647	0.58	P	350	0.58	P	360	0.78	P	486	4	RIKEN cDNA 1110030N17 gene
P	338	P	243	0.58	P	139	0.89	P	223	0.79	P	187	0.70	P	189	0.45	P	147	0.46	P	148	0.46	P	151	0.83	P	272	4	zinc finger protein 36
P	769	P	510	0.93	P	470	0.97	P	512	0.82	P	408	1.10	P	562	0.37	P	275	0.34	P	251	0.39	P	284	0.57	P	428	4	acetyl-Coenzyme A synthetase 2 (ADP for
P	185	P	112	1.51	P	186	0.54	P	82	0.95	P	103	1.67	P	186	0.44	P	79	0.30	P	54	0.57	P	101	0.66	P	118	4	similar to Isopentenyl-diphosphate delta-is
P	843	P	572	1.19	P	674	1.17	P	692	1.08	P	604	1.57	P	897	0.35	P	285	0.25	P	205	0.33	P	265	0.37	P	302	4	cytochrome P450, 8b1, sterol 12 alpha-hyd
P	83	P	57	1.76	P	98	1.34	P	79	0.85	P	53	1.64	P	93	0.42	P	34	0.51	P	41	0.43	P	35	0.39	P	31	4	carnitine palmitoyltransferase 1, liver
P	67	P	39	1.20	P	48	0.79	P	32	0.97	P	37	1.22	P	48	0.49	P	32	0.41	P	27	0.53	P	34	0.50	P	33	4	cytochrome P450, 51
P	310	P	191	1.17	P	221	0.84	P	128	1.28	P	239	1.58	P	302	0.32	P	98	0.32	P	95	0.41	P	121	0.55	P	165	4	squalene epoxidase
P	161	P	70	1.29	P	89	0.94	P	68	1.55	P	105	1.25	P	87	0.42	P	66	0.48	P	74	0.46	P	70	0.36	P	56	4	RIKEN cDNA 9830165K03 gene

Down-regulated

表 14　グリタゾン化合物による肝臓における CYP 関連遺伝子群の発現変化

	4OH				Tam				Tre				ΔC2H5			
	24h		4h		24h		4h		24h		4h		24h		4h	
CYP type	ratio	FlRaw	ratio	F Raw	ratio	F Raw	ratio	F Raw	ratio	F Raw	ratio	FlRaw	ratio	F Raw	ratio	FlRaw
Cyp17	0.91 P	691	0.82 P	694	1.27 P	958	1.20 P	1076	0.62 P	474	1.27 P	1090	1.17 P	895	1.02 P	887
Cyp1a2	0.53 P	940	0.99 P	1795	0.74 P	1311	0.95 P	1838	0.79 P	1407	0.87 P	1612	1.36 P	2451	0.97 P	1814
Cyp26a1	0.92 P	131	1.07 P	222	1.64 P	263	0.76 P	167	1.59 P	229	0.69 P	143	5.17 P	746	0.76 P	161
Cyp2b10	0.38 P	84	0.91 P	328	0.82 P	180	0.69 P	263	0.58 P	129	0.77 P	281	2.79 P	619	2.59 P	956
Cyp2b20	0.36 P	109	0.86 P	391	0.65 P	193	0.75 P	361	0.54 P	162	0.70 P	321	2.97 P	895	2.51 P	1176
Cyp2b20	0.38 A	83	1.13 P	407	0.85 A	186	0.79 M	302	0.49 A	108	0.77 P	281	3.00 P	664	2.44 P	897
Cyp2d9	0.75 P	304	1.64 P	704	0.63 P	256	0.86 P	392	1.15 P	470	1.14 P	494	1.68 P	689	1.05 P	462
Cyp2j5	0.42 P	94	0.62 P	110	0.75 P	169	1.05 P	198	1.01 P	227	0.58 P	106	0.97 P	219	0.89 P	163
Cyp2j6	1.40 P	63	0.57 A	41	0.81 P	36	0.46 A	36	1.35 P	61	0.73 P	54	1.02 P	46	0.64 P	48
Cyp4b1	0.48 P	67	1.01 P	125	0.71 P	99	0.97 P	128	0.50 P	70	0.80 P	101	0.80 P	112	0.88 P	112
Cyp51	0.51 P	134	1.14 P	123	0.35 P	92	0.87 P	100	0.48 P	128	1.35 P	148	0.56 P	150	1.73 P	191
Cyp51	0.53 P	34	0.97 P	37	0.41 P	27	0.79 P	32	0.49 P	32	1.20 P	46	0.50 P	33	1.22 P	48
Cyp7a1	0.44 P	186	0.97 P	305	0.43 P	181	0.68 P	227	0.36 P	151	0.63 P	202	0.81 P	343	1.30 P	419
Cyp7a1	0.52 P	506	1.25 P	943	0.46 P	447	0.72 P	579	0.40 P	398	0.76 P	583	0.97 P	961	1.32 P	1021
Cyp7b1	1.33 P	249	1.15 P	183	1.16 P	218	1.11 P	187	1.74 P	328	1.30 P	211	1.29 P	243	1.26 P	206
Cyp8b1	0.33 P	265	1.08 P	604	0.25 P	205	1.17 P	692	0.35 P	285	1.19 P	674	0.37 P	302	1.57 P	897

表 15　タモキシフェン誘導体処理により子宮において共通性をもって発現上昇した遺伝子

control		4OH	Tam	Tre	ΔC2Hs	4OH	Tam	Tre	ΔC2Hs	
4h	24h	4h				24h				Gene Name

F Raw	c	F Raw	OH4hr	F Raw	TAM4h	F Raw	Tore4h	F Raw	chem4h	F Raw	OH24hr	F Raw	TAM24h	F Raw	Tore24h	F Raw	chem24h	F Raw	sc	Description
A 20	M	24	48.62	P 897	55.04	P 914	2.88	0 P 72	18.54	P 303	144.63	P 3386	107.30	P 2716	104.68	P 2543	3.37	P 82	8	kallikrein 9
A 13	P	25	13.99	P 176	23.29	P 287	3.25	P 43	4.72	P 59	8.83	P 218	10.88	P 290	6.88	P 249	1.22	P 31	7	interleukin 1 receptor, type II
P 44	P	54	8.29	P 385	11.89	P 487	2.28	P 99	9.56	P 392	6.72	P 295	7.10	P 394	5.25	P 280	2.84	P 141	7	MAD2 (mitotic arrest deficient, homolog)-li
A 17	A	26	36.61	P 1534	129.00	P 1969	27.40	0 P 461	78.83	P 1250	69.93	P 1671	25.50	P 685	29.85	P 770	20.77	A 538	7	kallikrein 6
A 1	A	1	10.61	P 19	43.84	P 15	6.44	0 A 8	9.59	P 11	66.22	P 59	47.45	P 44	82.15	P 74	19.33	P 17	7	S100 calcium binding protein A14
P 40	P	60	4.28	P 181	8.01	P 223	1.32	A 52	4.57	P 163	4.61	P 279	6.27	P 387	5.49	P 325	0.94	P 56	6	desmocollin 2
P 27	P	31	5.10	P 127	5.71	P 165	1.47	P 39	6.41	P 159	9.03	P 266	7.79	P 247	9.57	P 261	1.09	P 33	6	desmocollin 2
P 92	P	86	8.91	P 765	7.15	P 603	1.62	P 146	7.06	P 600	2.83	P 235	3.85	P 344	4.35	P 373	0.89	P 76	6	GADD 45 gamma
P 38	P	73	3.24	P 116	6.15	P 181	1.08	P 41	3.75	P 133	3.57	P 251	2.46	P 186	3.25	P 237	0.66	P 48	6	galactose-4-epimerase, UDP
P 64	P	50	3.95	P 238	5.19	P 308	1.08	P 68	3.19	P 191	5.48	P 263	6.39	P 332	6.72	P 335	0.92	P 46	6	Jun dimerization protein 2
P 21	P	31	23.48	P 463	32.29	P 623	2.74	P 57	7.55	P 147	52.00	P 1549	59.09	P 1894	42.37	P 1304	1.06	P 33	6	kallikrein 14
P 25	P	28	9.24	P 87	5.38	P 122	1.05	P 26	5.76	P 133	4.53	P 121	8.54	P 159	14.03	P 387	1.46	P 41	6	similar to isopentenyl-diphosphate delta-is
P 248	P	372	3.67	P 854	5.01	P 1845	1.30	P 318	3.73	P 862	5.53	P 2107	5.85	P 2294	5.74	P 2124	0.84	P 311	6	peptidyl arginine deiminase, type II
P 158	P	269	11.95	P 1759	8.00	P 1166	1.60	P 249	7.56	P 1112	4.37	P 1134	8.73	P 1800	6.59	P 1498	0.87	P 233	6	purine-nucleoside phosphorylase
P 41	P	207	5.32	P 203	11.02	P 413	1.02	P 41	6.83	P 214	3.84	P 766	5.04	P 652	3.37	P 894	0.40	1 P 50	6	urate oxidase
A 16	P	46	6.82	P 104	43.07	P 195	0.51	0 A 8	4.32	P 65	8.70	P 379	6.21	P 385	7.04	P 317	0.27	1 A 12	6	apolipoprotein B editing complex 2
P 44	P	37	9.05	P 403	7.17	P 293	1.62	0 P 71	4.85	P 200	3.95	P 140	4.59	P 174	7.00	P 256	0.55	P 20	6	adult male diencephalon cDNAprotein
A 22	P	78	3.18	P 66	13.49	P 273	1.49	0 P 32	7.36	P 155	4.44	P 334	5.90	P 478	4.33	P 336	0.66	P 51	6	RIKEN cDNA A930031D07 gene
A 42	A	58	17.48	P 681	18.17	P 695	2.38	0 A 97	6.65	P 253	31.92	P 1769	24.65	P 1483	15.88	P 908	0.63	A 37	6	kallikrein 21
P 262	P	491	3.08	P 759	5.90	P 1427	1.07	0 P 277	3.20	P 781	3.22	P 1524	3.75	P 1457	3.90	P 1806	0.83	P 409	6	keratin complex 2, basic, gene 7
A 3	P	19	65.17	P 80	84.36	P 156	1.30	0 A 4	26.89	P 64	4.91	P 88	7.65	P 148	12.82	P 237	0.83	P 16	6	stratifin
P 32	P	23	4.91	P 149	4.78	P 142	1.12	0 P 36	3.56	P 107	3.63	P 80	5.88	P 136	4.40	P 99	0.99	P 22	6	paired related homeobox 2
P 215	P	156	3.82	P 582	3.96	P 785	1.12	0 P 237	3.86	P 778	5.03	P 892	7.43	P 1201	7.55	P 1172	1.43	P 223	6	aldehyde dehydrogenase family 1, subfamily
P 27	P	31	4.08	P 104	3.94	P 99	1.77	P 47	4.50	P 114	3.32	P 98	2.13	P 68	3.91	P 119	1.73	P 53	5	RIKEN cDNA 2610307C23 gene
P 22	P	30	3.45	P 70	4.78	P 95	1.24	P 26	3.74	P 75	2.38	P 69	3.09	P 114	7.24	P 220	1.07	P 32	5	cytochrome P450, 51
P 86	P	91	1.72	P 139	3.83	P 288	0.99	P 84	3.62	P 289	2.74	P 241	5.70	P 536	5.79	P 521	2.15	P 195	5	farnesyl diphosphate synthetase
P 118	P	81	2.17	P 241	1.91	P 208	1.24	P 144	2.96	P 325	4.23	P 331	3.52	P 296	3.82	P 308	2.79	P 226	5	karyopherin (importin) alpha 2
P 53	P	78	3.98	P 197	8.08	P 248	1.30	P 68	4.65	P 231	2.36	P 178	3.91	P 317	4.63	P 360	1.01	P 79	5	low density lipoprotein receptor
P 430	P	704	5.82	P 2352	8.56	P 2594	1.39	P 588	5.38	P 2151	3.68	P 2468	2.51	P 1835	2.55	P 1788	0.92	P 649	5	purine-nucleoside phosphorylase
P 22	P	48	6.72	P 200	9.69	P 74	3.16	P 68	5.76	P 138	3.65	P 162	0.40	P 19	0.54	P 25	1.04	P 48	5	ribosomal protein L37a
P 21	P	44	4.00	P 77	6.41	P 102	1.11	P 22	6.30	P 101	1.62	P 69	4.71	P 124	5.61	P 389	0.65	P 29	5	sterol-C4-methyl oxidase-like
P 202	P	223	8.41	P 1025	3.24	P 620	2.01	P 399	4.64	P 875	0.75	P 180	2.50	P 578	2.70	P 599	1.10	P 245	5	splicing factor, arginine/serine-rich 2
P 28	P	28	3.63	P 96	3.32	P 86	0.95	P 26	4.47	P 117	3.55	P 95	2.51	P 73	3.20	P 89	2.05	P 57	5	splicing factor, arginine/serine-rich 2
P 236	P	311	2.87	P 837	3.82	P 832	1.02	P 236	3.06	P 659	2.89	P 775	2.33	P 750	2.82	P 902	0.81	P 251	5	testis expressed gene 2
P 114	P	156	4.43	P 473	6.55	P 686	1.29	P 144	2.97	P 314	3.66	P 397	2.33	P 376	2.81	P 450	0.94	P 146	5	neurturin
P 32	P	37	3.15	P 100	3.45	P 101	1.20	P 38	2.41	P 71	3.03	P 109	3.22	P 124	4.50	P 167	0.99	P 37	5	Nedd4 WW binding protein 4
P 58	P	23	3.65	P 202	4.21	P 229	1.30	P 75	2.19	P 120	5.59	P 123	4.72	P 206	8.19	P 141	2.69	P 61	5	crystallin, alpha B
P 61	P	61	1.46	P 83	8.00	P 336	0.81	A 49	3.71	P 209	10.93	P 639	10.24	P 644	12.63	P 782	1.04	P 63	5	RIKEN cDNA A930031D07 gene
M 11	A	8	0.43	M 4	0.60	A 6	1.55	P 17	3.69	P 37	8.05	P 69	9.29	P 76	5.87	P 45	7.41	P 59	5	protein regulator of cytokinesis 1-like
A 10	A	22	10.00	P 90	8.76	P 77	2.49	A 24	12.45	P 111	2.09	A 44	2.98	P 67	3.90	P 65	0.37	A 8	5	a disintegrin-like and metalloprotease
A 13	A	8	18.49	P 226	13.12	P 157	1.94	A 25	14.33	P 173	2.53	A 19	10.75	P 168	19.45	P 151	0.44	A 3	5	TNF receptor superfamily, member 12a
P 24	P	45	3.91	P 227	12.78	P 287	2.24	P 54	7.55	P 171	2.72	P 118	4.65	P 217	4.87	P 218	0.89	P 40	5	Nedd4 WW binding protein 4
P 536	P	565	2.05	P 1505	2.50	P 1728	1.18	P 624	3.03	P 1510	2.11	P 1150	2.96	P 1734	3.61	P 2030	1.16	P 855	5	receptor (calcitonin) activity modifying prot
P 116	A	130	5.23	P 567	9.00	P 383	1.10	M 125	3.37	P 899	1.31	P 183	2.79	P 375	3.46	P 446	1.10	P 142	5	serum-inducible kinase
P 41	P	56	4.73	P 184	5.38	P 205	1.40	P 57	4.41	P 170	2.27	P 123	3.24	P 189	3.08	P 173	1.03	P 58	5	melanophilin
A 24	A	27	3.91	P 80	3.29	P 74	1.83	A 44	3.23	P 73	2.80	P 74	3.78	P 108	3.33	P 81	0.92	A 25	5	rat proto-oncogene
P 67	P	66	7.16	P 450	4.56	P 282	2.16	P 143	6.82	P 350	1.91	P 126	4.38	P 237	6.71	P 252	1.20	P 82	5	chemokine orphan receptor 1
P 13	A	12	8.54	P 67	5.56	P 86	1.22	A 15	5.16	P 82	3.76	A 43	3.61	P 47	5.35	P 63	0.87	A 10	5	histamine receptor H 1
A 22	P	21	7.07	P 148	7.06	P 146	2.25	P 49	10.68	P 221	2.74	P 55	5.93	P 128	4.51	P 93	1.03	A 22	5	a disintegrin-like and metalloprotease
P 21	P	19	6.29	P 127	4.85	P 94	1.14	P 24	4.46	P 88	3.32	M 60	6.90	P 134	7.48	P 139	1.02	A 19	5	parathyroid hormone-like peptide
P 8	P	8	6.00	P 82	7.02	P 54	1.78	P 15	4.13	P 32	6.03	M 47	6.47	P 54	5.42	P 43	0.86	P 7	5	parathyroid hormone-like peptide
A 22	A	7	13.85	P 286	10.46	P 212	0.56	A 12	12.53	P 256	9.11	A 61	20.14	P 216	21.93	P 219	0.93	A 6	5	TNF receptor superfamily, member 12a

表 16　タモキシフェン誘導体処理により子宮において共通性をもって発現低下した遺伝子

control		4OH	Tam	Tre	ΔC2Hs	4OH	Tam	Tre	ΔC2Hs	
4h	24h	4h				24h				Gene Name

F Raw	c	F Raw	OH4hr	F Raw	TAM4h	F Raw	Tore4h	F Raw	chem4h	F Raw	OH24	F Raw	TAM24h	F Raw	Tore24h	F Raw	chem24h	F Raw	score	Description
P 173	P	91	0.23	P 37	0.14	P 23	0.94	P 159	0.35	P 57	0.30	A 26	0.21	P 20	0.16	P 15	1.20	P 109	6	N-sulfotransferase
P 350	P	489	0.35	P 114	0.31	P 101	0.93	P 321	0.24	P 79	0.24	P 112	0.38	P 192	0.24	P 118	1.26	P 615	6	D site albumin promoter binding protein
P 534	P	326	0.32	P 160	0.29	P 142	0.72	P 378	0.39	P 195	0.41	P 128	0.37	P 126	0.31	P 101	0.94	P 306	6	glucocorticoid-induced leucine zipper
P 186	P	93	0.40	A 70	0.19	A 33	0.87	P 159	0.38	A 62	0.13	A 12	0.25	A 24	0.09	A 8	1.15	P 106	6	flavin containing monooxygenase 2
P 820	P	781	0.85	P 190	0.24	P 182	0.98	P 791	0.37	P 284	0.32	P 240	0.23	P 183	0.26	P 204	1.14	P 891	6	REV3-like
P 49	P	37	0.38	P 16	0.26	P 12	1.24	P 59	0.26	P 13	0.03	A 1	0.09	P 4	0.25	A 9	1.75	P 65	6	carbonic anhydrase-like sequence 1
P 63	P	35	0.38	A 21	0.15	A 9	0.99	P 61	0.20	A 12	0.15	A 5	0.05	A 2	0.18	A 6	1.06	P 37	6	claudin 1
P 80	P	79	0.26	P 22	0.20	P 15	0.35	P 28	0.46	P 35	0.23	P 18	0.29	P 24	0.35	P 27	1.20	P 94	6	RIKEN cDNA 2610002J02 gene
P 370	P	804	0.25	P 85	0.20	P 68	1.00	P 384	0.23	P 78	0.24	P 142	0.25	P 156	0.24	P 144	1.31	P 794	6	D site albumin promoter binding protein
P 483	P	481	0.32	P 150	0.22	P 98	0.89	P 432	0.31	P 142	0.24	P 107	0.23	P 110	0.17	P 76	0.99	P 457	6	secreted frizzled-related sequence protein
P 63	P	36	0.24	A 14	0.13	A 8	0.81	P 51	0.34	A 20	0.05	A 2	0.09	A 3	0.15	A 5	1.18	P 42	6	prostaglandin E receptor 2 (subtype EP2)
P 264	P	313	0.19	P 46	0.35	P 85	0.78	P 204	0.36	P 89	0.36	P 110	0.35	P 114	0.32	P 100	0.83	P 260	6	Max interacting protein 1
P 282	P	307	0.14	P 36	0.29	P 75	1.04	P 289	0.21	P 54	0.21	P 63	0.36	P 115	0.29	P 87	1.07	P 328	6	Cbp/p300-interacting transactivator
P 938	P	1221	0.28	P 243	0.40	P 347	0.91	P 636	0.25	P 221	0.23	P 271	0.39	P 490	0.11	P 133	1.03	P 1260	5	thioredoxin interacting protein
P 40	P	83	0.46	A 17	0.07	A 3	0.35	P 14	1.03	P 38	0.19	A 15	0.22	P 19	0.39	P 24	0.40	P 26	5	neutral sphingomyelinase activation associ
P 110	P	118	0.22	P 30	0.15	P 15	0.83	P 90	0.64	P 66	0.31	P 35	0.18	P 22	0.12	P 13	0.59	P 58	5	RIKEN cDNA E330010H22 gene
P 61	P	59	0.09	A 5	0.17	A 9	1.00	P 60	0.37	A 21	0.18	A 10	0.44	P 27	0.20	A 12	1.05	P 62	5	RIKEN cDNA 4632432J16 gene
P 61	P	47	0.33	A 19	0.32	A 18	1.03	P 61	0.32	A 18	0.33	A 15	0.39	A 19	0.30	A 14	2.14	P 101	5	growth factor receptor bound protein 14
P 193	P	284	0.67	P 122	0.42	P 76	1.03	P 195	0.38	P 64	0.17	A 45	0.17	P 49	0.13	P 37	1.63	P 462	5	RIKEN cDNA 1200011D03 gene
P 203	P	152	0.28	P 49	0.32	P 59	0.86	P 171	0.30	P 57	0.58	P 85	0.28	P 44	0.36	P 54	1.29	P 196	5	hydroxyprostaglandin dehydrogenase 15 (N
P 146	P	97	0.34	P 47	0.31	P 41	1.14	P 163	0.35	P 47	0.06	A 6	0.62	P 62	0.28	P 27	1.40	P 137	5	regulator of G-protein signaling 5
P 802	P	958	0.54	P 302	0.28	P 157	1.08	P 640	0.37	P 208	0.23	P 210	0.26	P 256	0.21	P 197	0.86	P 631	5	ATP-binding cassette, sub-family A (ABC1
P 301	P	324	0.35	P 100	0.51	P 141	0.74	P 219	0.33	P 92	0.18	P 56	0.28	P 95	0.23	P 76	0.85	P 278	5	insulin-like growth factor binding protein 3
P 105	P	147	0.19	A 19	0.01	P 20	0.85	P 88	0.28	P 27	0.39	P 55	0.34	P 51	0.28	P 41	0.85	P 125	5	RIKEN cDNA 2310014B08 gene
P 81	P	269	0.29	A 22	1.21	P 90	0.68	P 54	0.32	A 24	0.10	A 25	0.10	P 28	0.13	P 36	0.37	P 99	5	immunoglobulin lambda chain, variable 1
P 397	P	192	0.24	P 88	0.22	P 80	0.72	P 280	0.24	P 87	0.38	P 71	0.49	P 98	0.29	P 55	1.12	P 215	5	glucocorticoid-induced leucine zipper
P 81	P	91	0.55	P 42	0.21	P 18	0.82	P 65	0.36	P 27	0.03	A 2	0.13	P 13	0.11	P 10	1.18	P 108	5	leptin receptor
P 522	P	356	0.21	P 105	0.01	P 64	0.94	P 482	0.18	P 88	0.14	P 47	0.29	P 106	0.12	P 43	1.10	P 390	5	odd-skipped related 2 (Drosophila)
P 379	P	254	0.09	A 32	0.01	A 18	1.00	P 373	0.15	P 53	0.26	A 65	0.09	A 24	0.15	P 39	1.04	P 264	5	RIKEN cDNA 9930023K05 gene
P 157	P	321	0.56	P 82	0.42	P 81	0.86	P 147	0.36	P 55	0.28	P 87	0.20	P 67	0.26	P 84	0.64	P 204	5	viral hemorrhagic septicemia virus(VHSV) i
P 272	P	260	0.55	P 140	0.32	P 81	1.00	P 269	0.42	P 107	0.06	A 16	0.19	P 52	0.09	A 22	1.43	P 372	5	ectonucleotide pyrophosphatase/phosphod
P 314	P	344	0.09	A 26	0.01	P 28	0.97	P 296	0.12	P 34	0.22	P 73	0.30	P 106	0.17	P 58	0.84	P 288	5	F-box only protein 32
P 84	P	47	0.23	A 18	0.17	P 13	1.01	P 83	0.28	P 22	0.52	A 28	0.26	P 13	0.29	P 14	1.12	P 53	5	Norrie disease homolog
P 132	P	139	0.35	P 43	0.01	P 27	0.84	P 108	0.26	P 32	0.26	P 35	0.27	P 38	0.27	P 38	0.98	P 135	5	caspase 12
P 630	P	810	0.27	P 159	0.01	P 155	0.87	P 538	0.36	P 209	0.38	P 224	0.26	P 168	0.18	P 109	1.04	P 634	5	RIKEN cDNA 4933425F03 gene
P 283	P	137	0.25	P 62	0.10	P 23	0.77	P 199	0.21	P 51	0.16	A 22	0.55	P 78	0.66	P 90	0.40	P 49	5	receptor (calcitonin) activity modifying prot
P 529	P	293	0.38	P 189	0.07	P 32	0.94	P 487	0.06	P 37	0.13	A 38	1.07	P 326	0.53	P 155	0.40	P 104	5	receptor (calcitonin) activity modifying prot

表17　タモキシフェン誘導体処理したマウス子宮でのエストロジェンレセプター関連遺伝子群の発現変化

4OH				Tam				Tre				Δ C2H5				Gene	
4hr	FIRaw	24hr	FIRaw	4hr	F Raw	24hr	F Raw	4hr	F Raw	24hr	F Raw	4hr	F Raw	24hr	F Raw	Common	Description
0.33 P	118	0.71 P	351	0.73 P	251	0.60 P	317	0.86 P	317	0.76 P	390	0.51 P	179	0.69 P	354	Trim25	tripartite motif protein 25(efp)
2.20 P	1939	0.87 P	4438	2.77 P	2390	0.47 P	2614	0.99 P	816	0.30 P	1599	0.97 P	847	0.32 P	1697	Ltf	lactotransferrin
1.64 P	578.4	1.95 P	594.4	1.45 P	502.4	0.8 P	260.7	1.34 P	494.2	0.72 P	228.2	1.74 P	607.9	1.04 P	328.7	TFF1	trefoil factor 1(breast cancer estrogen-inducible sequ
1.18 P	884.7	2.24 P	2424	2.17 P	1591	1.8 P	2128	0.9 P	702	2.09 P	2337	1.44 P	1067	1.14 P	1278	KRT1-	keratin19
0.41 A	7	0.71 A	15	0.43 A	7	0.57 P	13	1.19 A	21	0.28 A	8	0.57 A	10	0.85 P	19	Hgf	hepatocyte growth factor
3.02 P	82	3.67 A	87	2.00 A	40	2.34 P	46	1.19 A	25	1.41 M	27	2.71 A	55	1.30 A	25	Oxtr	Mus sp. mRNA for oxytocin receptor, complete cds.
1.21 P	1599	1.39 P	6788	3.15 P	4100	0.68 P	3567	0.96 P	1332	0.50 P	2543	1.29 P	1892	0.40 P	2028	C3	complement component 3
3.28 P	1879	2.45 P	1327	7.88 P	4427	0.76 P	4442	1.00 P	602	0.70 P	3889	3.84 P	2004	0.40 P	1367	Lcn2	lipocalin 2
0.36 P	798	0.85 P	967	0.46 P	994	0.68 P	835	1.00 P	2336	0.76 P	894	0.78 P	1715	0.81 P	962	Ctsd	cathepsin D
0.56 A	49	0.79 A	53	0.43 A	37	0.84 M	81	1.11 M	102	0.44 A	31	0.40 A	35	1.13 P	79	Vegfb	vascular endothelial growth factor B
0.07 A	2	0.39 A	8	0.01 A	6	0.56 A	12	0.88 A	26	0.70 P	15	0.31 A	9	1.36 P	29	Vegfc	vascular endothelial growth factor C
2.7 P	83.9	0.87 P	45.7	1.73 P	52.8	0.9 P	49.7	1.49 P	48.6	1 P	54.1	1.5 P	46	1.02 P	55.2	Tgfa	transforming growth factor, alpha
0.81 P	94	0.30 A	34	0.68 P	77	0.52 P	63	0.60 P	73	0.38 P	44	0.53 P	81	1.41 P	165	Tgfb3	transforming growth factor, beta 3
2.00 P	32	0.34 A	1	2.58 P	41	1.28 P	22	1.17 P	20	3.06 P	50	2.87 P	46	0.96 P	16	Hmgcr	3-hydroxy-3-methylglutaryl-Coenzyme A reductase
2.19 P	107.1	2.04 P	59.2	1.61 P	77.1	2.3 P	72.2	1.07 P	54.6	1.34 P	40	1.68 P	81.3	1.53 P	46.1	PGR	progesterone receptor
2.20 A	47	0.83 A	36	0.01 A	7	1.07 P	50	2.40 A	54	0.26 A	11	1.04 A	22	1.13 P	51	Esr1	estrogen receptor 1 (alpha)
0.85 P	110.6	0.95 P	110.5	0.7 P	90.3	1 P	129.7	1 P	136.1	1.13 P	135.7	0.74 P	95.3	0.98 P	118.7	EBAG9	estrogen receptor-binding site-associated antigen 9
0.57 P	188	0.68 A	160	0.43 M	139	1.07 P	271	0.91 P	312	0.55 P	134	0.55 P	177	1.58 P	385	Igfbp4	insulin-like growth factor binding protein 4
1.10 P	310	4.81 P	582	1.39 P	384	3.49 P	753	1.08 P	321	2.89 P	491	2.14 P	599	1.95 P	281	Igf1	insulin-like growth factor 1
1.16 P	194	2.19 P	220	1.24 P	204	2.26 P	391	1.06 P	186	1.19 P	223	2.25 P	372	2.49 P	178	Igf1	insulin-like growth factor 1
0.50 A	63	0.35 A	50	0.91 P	45	0.46 P	66	1.02 P	135	0.23 P	32	0.43 P	53	0.76 P	105	Igf1r	insulin-like growth factor I receptor
2.16 A	30	5.21 P	75	1.03 A	14	2.13 P	33	0.39 A	6	2.75 P	41	1.52 A	21	1.02 P	15	E2f1	E2F transcription factor 1
3.66 P	197	2.36 P	178	5.09 P	248	3.91 P	317	1.30 P	88	4.63 P	360	4.86 P	231	1.01 P	79	Ldlr	low density lipoprotein receptor
3.96 P	197	2.36 P	178	8.09 P	248	3.91 P	317	1.30 P	88	4.63 P	360	4.69 P	231	1.01 P	79	Ldlr	low density lipoprotein receptor
5.41 P	443	1.01 P	276	5.18 P	417	0.69 P	262	1.42 P	121	1.25 P	354	6.05 P	492	0.43 P	122	Fos	FBJ osteosarcoma oncogene
0.88 A	68	0.67 A	33	0.55 A	42	0.93 P	49	0.92 P	75	0.23 A	12	0.69 A	53	1.36 P	69	Bcl2	B-cell leukemia/lymphoma 2
1.84 P	564.4	1.82 P	476.5	1.75 P	526.8	1.7 P	480	0.96 P	313.9	2.13 P	578	1.91 P	578	1.06 P	287.8	cend1	
1.84 P	279.4	1.51 P	195.1	2.05 P	306.5	2.3 P	322.7	1.48 P	236.3	2.01 P	267.5	2.24 P	338	0.92 P	122.4	cend1	
1.29 P	80.3	1.3 A	52.1	1.79 P	82.2	1.8 P	70.5	1.17 P	57.4	2.01 P	83.4	1.81 P	84.1	0.93 P	38.6	cend1	
1.43 P	317.8	1.74 P	344	1.18 P	257.3	1.7 P	360.9	1.1 P	254.4	1.39 P	283.4	1.44 P	315.8	1.04 P	212.1	cend3	
0.44 P	17	1.48 A	32	0.88 P	33	3.96 P	91	0.93 P	37	3.78 P	83	1.00 P	38	2.42 P	53	Serpinb1a	ovalbumin
1.8 P	108	0.39 A	2.8	1.53 P	9	0.4 A	3	1.34 P	8.4	0.22 A	1.5	1.33 A	7.9	0.41 A	2.8	DL8	
0.90 M	14	4.24 P	40	0.83 A	12	4.04 P	41	1.39 P	22	5.16 P	50	1.83 P	28	2.77 P	27	Brca1	breast canbreast cancer 1
0.59 P	138	0.45 A	78	0.43 P	99	0.54 P	102	1.02 P	247	0.27 P	64	0.79 P	182	0.78 P	138	Myc	myelocytomatosis oncogene
1.57 P	78	1.74 P	273	0.24 P	257	1.73 P	292	1.43 P	75	2.28 P	370	2.70 P	134	0.86 P	139	Ckmt1	creatine kinase, mitochondrial 1, ubiquitous
1.82 P	121.8	1.69 P	67.6	1.5 P	98.9	1.7 P	72.6	0.8 P	56.1	1.37 P	58.6	1.27 P	84.2	0.95 P	39.5	NOS3	eNOS
0.83 P	44	0.30 P	112	0.48 P	25	0.36 P	144	1.11 P	82	0.33 P	128	0.52 P	27	0.67 P	260	Mmp11	matrix metalloproteinase 11
0.88 P	101	0.37 P	57	0.68 P	76	0.93 P	153	0.89 P	107	0.48 P	74	0.79 P	90	0.94 P	149	Mmp14	matrix metalloproteinase 14 (membrane-inserted)
0.60 A	17	1.78 A	31	0.26 A	7	3.18 P	58	0.76 A	22	4.76 P	84	0.15 A	4	1.28 P	23	Mmp15	matrix metalloproteinase 15
1.58 P	57	3.81 P	134	1.91 P	68	1.59 P	63	1.43 P	54	1.33 P	51	1.54 P	55	1.12 P	43	Mmp17	matrix metalloproteinase 17
2.91 M	74	3.90 A	60	0.79 P	20	2.93 P	48	1.31 M	35	1.91 P	30	1.51 P	38	2.33 P	37	Mmp19	matrix metalloproteinase 19
0.72 A	19	0.16 A	7	1.01 A	28	0.18 A	8	0.90 A	24	0.11 A	5	0.83 A	21	0.50 A	23	Mmp3	matrix metalloproteinase 3
4.11 P	198	1.04 A	194	2.77 A	127	0.66 P	133	0.89 A	43	0.80 P	154	1.30 A	60	0.23 A	45	Mmp7	matrix metalloproteinase 7
0.69 A	33	0.34 P	153	2.24 P	152	0.72 P	321	0.99 A	50	0.27 P	147	1.92 P	91	0.40 P	121	Ceacam1	CEA-related cell adhesion molecule 1
1.12 A	37	0.34 A	37	1.82 P	59	0.45 P	63	1.35 A	47	0.27 P	29	2.37 A	78	0.40 P	42	Ceacam1	CEA-related cell adhesion molecule 1
1.08 P	269	0.89 P	820	2.36 P	574	0.68 P	854	1.02 P	264	0.53 P	651	1.50 P	368	0.40 P	386	Ceacam2	CEA-related cell adhesion molecule 2
0.91 P	157	0.83 P	541	2.21 P	378	0.56 P	523	0.87 P	157	0.44 P	388	1.46 P	251	0.40 P	278	Ceacam2	CEA-related cell adhesion molecule 2
0.40 A	70	0.34 A	12	0.19 A	33	0.25 A	24	0.87 P	159	0.27 A	8	0.36 A	62	1.15 P	106	Fmo2	flavin cont flavin-containing monooxygenase 2
0.43 A	53	0.41 A	27	0.28 M	34	0.24 M	17	0.78 P	100	0.27 A	2	0.17 A	21	0.73 P	50	Fmo2	flavin cont flavin-containing monooxygenase 2
0.93 P	116	0.34 A	25	0.59 P	72	0.74 P	110	0.89 P	90	0.27 A	15	0.58 P	69	1.38 P	197	26st	interleukin 6 signal transducer
0.55 A	44	1.00 A	134	0.53 P	42	0.51 P	74	1.57 P	132	0.27 A	32	0.65 M	52	0.40 P	48	Tiarp-pendin	Tnfa-induced adipose-related protein
2.43 P	40	0.34 A	19	2.05 P	33	0.48 P	33	1.09 P	19	0.42 P	27	2.17 P	36	0.40 P	15	Tnfaip2	tumor necrosis factor, alpha-induced protein 2
0.95 A	3	0.34 A	0	0.12 A	0	0.66 A	3	1.40 P	5	0.45 A	2	1.37 A	5	1.16 M	4	Tnfrsf11b	tumor necrosis factor receptor superfamily, member 1
0.27 P	34	0.48 P	57	0.01 P	33	0.22 P	28	1.03 P	134	0.35 P	43	0.24 P	29	1.34 P	165	Tnfrsf19	tumor necrosis factor receptor superfamily, member 1
0.15 A	5	0.28 A	7	0.52 A	16	0.24 A	6	0.80 A	26	0.41 A	10	0.68 A	3	1.29 P	32	Tnfrsf19	tumor necrosis factor receptor superfamily, member 1
0.31 P	48	0.53 A	73	0.01 P	83	0.64 P	95	0.95 P	149	0.88 P	94	0.38 P	56	0.88 P	98	Tnfrsf21	expressed sequence AA959878
1.33 P	163	1.81 P	199	1.32 P	159	1.91 P	254	1.02 P	131	2.84 P	383	1.29 P	157	0.99 P	127	Ap1s1	adaptor protein complex AP-1, sigma 1
0.93 P	91	0.81 P	98	1.29 P	123	0.52 P	89	1.32 P	134	0.27 P	90	1.04 P	100	0.74 P	123	Stat1	signal transducer and activator of transcription 1
0.90 P	35	0.34 P	21	0.86 P	33	0.45 P	32	0.78 P	31	0.27 P	18	0.67 P	26	0.63 P	43	Stat2	signal transducer and activator of transcription 2
1.49 P	57	0.34 A	8	1.54 P	58	1.75 P	55	0.80 P	32	0.72 P	22	1.28 P	49	1.32 P	40	Stat5a	signal transducer and activator of transcription 5A

ERE-dependent genomic action　　ERE-independent genomic action　　non-genomic action

表18　タモキシフェン誘導体処理したマウス子宮での遺伝子傷害関連遺伝子群の発現変化

4OH				Tam				Tre				ΔC2H5				Gene
4hr	FIRaw	24hr	FIRaw	4hr	FIRaw	24hr	FIRaw	4hr	FIRaw	24hr	FIRaw	4hr	FIRaw	24hr	FIRaw	Description
1.13 P	78	4.63 P	401	1.70 P	116	2.90 P	270	1.00 P	73	3.62 P	324	1.59 P	110	0.41 P	37	fatty acid binding protein 5, epidermal
3.02 P	155	1.65 P	143	3.92 P	198	0.92 P	86	1.37 A	74	1.38 P	123	2.89 P	147	0.67 M	60	cyclin-dependent kinase inhibitor 1A (P21)
1.87 P	136	2.36 P	192	3.09 P	220	2.43 P	212	1.38 P	105	2.68 P	223	2.62 P	188	0.69 P	58	pleckstrin homology-like domain, family A member 1
1.59 P	261	2.62 P	312	1.93 P	312	2.64 P	338	1.18 P	203	2.63 P	323	1.53 P	248	1.08 P	133	pleckstrin homology-like domain, family A member 3
2.42 P	815	2.33 P	563	2.04 P	675	2.72 P	708	0.91 P	320	4.98 P	1243	1.37 P	457	1.06 P	266	RIKEN cDNA 5830413E08 gene
1.14 P	259	1.51 P	322	1.43 P	318	2.80 P	598	1.10 P	261	2.58 P	569	1.50 P	337	1.12 P	248	RIKEN cDNA 1700037B15 gene
0.68 A	36	3.93 P	223	1.35 P	70	2.97 P	181	0.91 P	50	2.47 P	145	0.61 A	32	1.19 P	70	growth arrest and DNA-damage-inducible 45 gamma
0.53 P	205	0.81 P	145	0.62 P	236	2.57 P	496	0.89 P	364	0.14 A	26	0.50 P	193	0.54 P	101	carbonic anhydrase 3
2.89 P	226	1.71 P	125	2.06 P	158	1.03 P	81	1.18 P	97	1.25 P	94	2.21 P	171	0.66 P	50	RIKEN cDNA 2700083B06 gene
2.26 P	141	0.91 P	87	2.23 P	137	2.07 P	214	1.01 P	66	2.71 P	268	1.57 P	97	0.73 P	73	sterol-C5-desaturase (fungal ERG3, delta-5-desaturase) homol
3.10 P	78	0.25 A	8	2.90 A	60	0.73 A	25	1.55 A	35	0.68 A	22	2.65 A	56	0.72 A	23	growth differentiation factor 15
2.73 P	1659	1.43 P	710	1.71 P	1019	1.44 P	767	1.22 P	777	1.49 P	759	2.33 P	1401	1.14 P	586	heat shock protein, 1
0.65 P	55	2.85 P	70	0.61 P	50	1.56 P	40	1.11 P	98	0.35 P	8	0.57 P	48	1.02 P	25	ESTs, Highly similar to 2118318A promyelocyte leukemia Zn fing
0.21 A	10	2.12 A	14	0.04 A	2	4.08 P	28	1.25 P	64	0.88 A	6	0.62 A	30	0.77 A	5	ESTs, Highly similar to 2118318A promyelocyte leukemia Zn fing
1.06 P	183	0.69 P	231	1.02 P	173	0.39 P	139	1.28 P	231	0.58 P	200	1.32 P	225	0.56 P	195	B-cell translocation gene 2, anti-proliferative
1.10 P	235	0.22 A	71	1.89 P	398	1.83 P	617	1.15 P	258	0.22 P	70	1.34 P	286	0.87 P	283	RIKEN cDNA 1300007C21 gene
0.47 P	75	0.53 P	44	0.34 P	52	0.47 P	42	1.31 P	217	0.33 P	29	0.48 P	75	0.85 P	73	RIKEN cDNA 1110002J03 gene
0.27 P	159	0.38 P	224	0.27 P	155	0.28 P	168	0.87 P	538	0.18 P	109	0.36 P	209	1.04 P	634	RIKEN cDNA 4933425F03 gene
0.67 A	20	0.57 A	32	0.79 A	23	0.57 P	34	1.10 P	35	0.16 A	9	0.57 A	17	0.91 P	54	stress induced protein
0.55 P	70	1.09 P	123	0.69 P	85	0.92 P	111	0.92 P	121	0.24 P	27	0.76 P	94	2.21 P	257	insulin-like growth factor binding protein 5

図３　発現強度のスキャタープロットと発現強度に応じた段階的遺伝子選択法

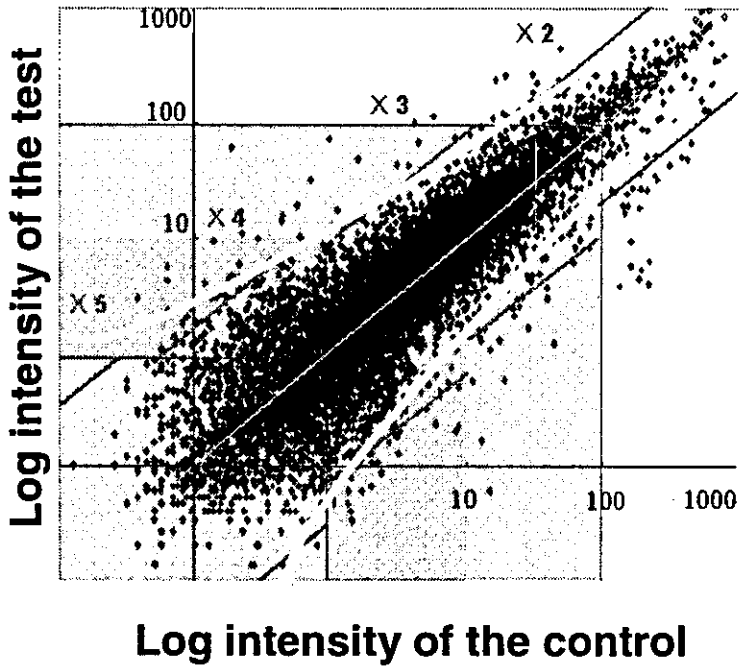

図４　遺伝子発現データベースの構造

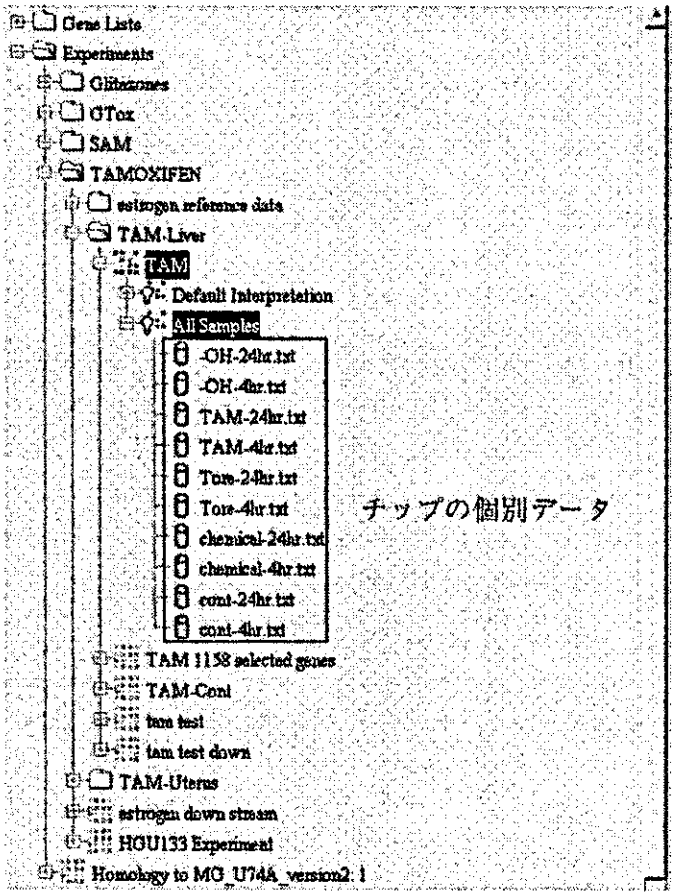

図5　ヒトデータとマウスデータの直接比較法（HU133A から MOE430 への変換の例）

1. Excel にて HU133A MOE430 アレイのプローブ ID をリストアップした表を作成。

	A	B
1	221517_s_a	1451719_at
2	209708_at	1422643_at
3	221407_at	1423019_at
4	214886_s_a	1417707_at
5	204843_s_a	1452915_at
6	202780_at	1428140_at

2. このファイルを MOE430.homology という名前で、GeneSpring の HU133 チップフォルダー内にある "Homology Tables" というフォルダーへ保存する。

3. これにより、自動的に HU133A チップでの遺伝子リストをマウスのゲノムへ変換するための準備が整うが、GeneSpring 上で変換操作を行うと、両者のデータは横並びには表示されず、対応するマウスのチップ上のプローブ ID のみが右のように表示される。

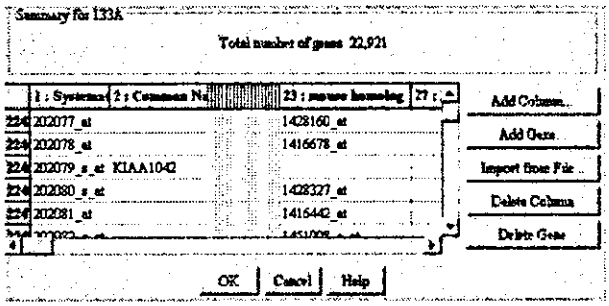

4. 次に mouse homolog ID を含む HU133A データを表形式で Excel 上へ書き出すと右の表の左側の赤色で示した部分に mouse homolog（青色）が追加される。

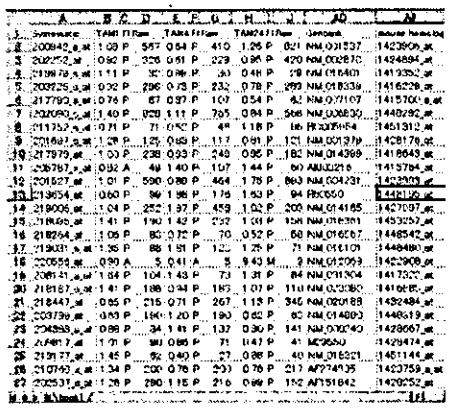

5. 次に、この mouse homolog を用いて MOE430 用の遺伝子リストを作成し、GeneSpring 上にて対応するマウスチップのデータから対応するデータをリストアップし、同様に Excel 上へ転送する。

6. Mouse homolog の項をキーとして HU133A および MOE430 のデータを並び替え、一部重複する項目を手作業にて整理することにより両者を一つの Excel ファイル上で横並びの表として結合させる。これにより、両者のデータを用いてスキャタープロットを書かせるなどの直接比較が可能となる。

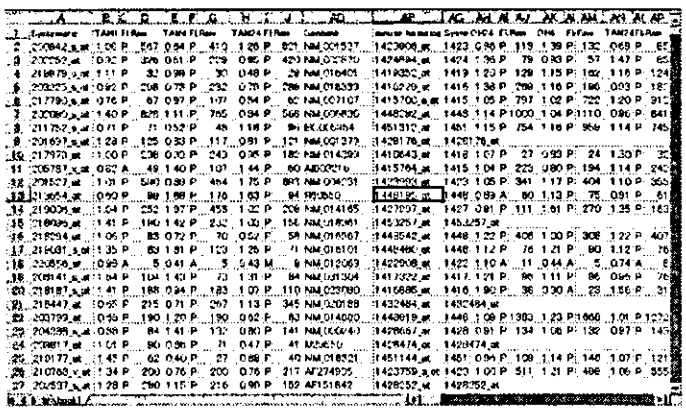

図6　タモキシフェン処理ヒト肝初代培養細胞でのデータとマウス肝臓でのデータの直接比較

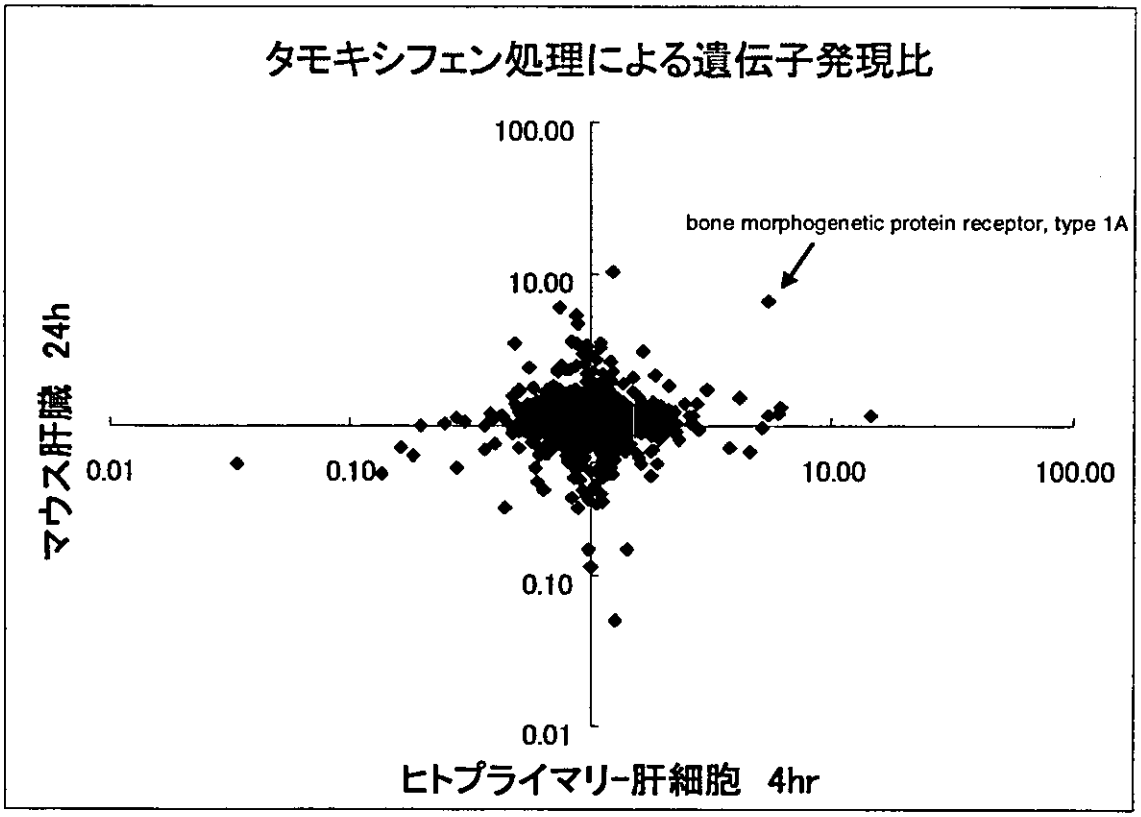

表19　グリタゾン化合物処理による in vivo(マウス)と in vitro(ヒト)データの共通性の比較

Mouse in vivo																								Human in vitro												
IP2D	IR2D	IT2D	IP2H	IR2H	IT2H	4P2D	4R2D	4T2D	4P2H	4R2H	4T2H	24PL	24RL	24TL	24PH	24RH	24TH	72PL	72RL	72TL	72PH	72RH	72TH	IP	IR	IT	4P	4R	4T	24P	24R	24T	72P	72R	72T	Description
1.76	1.75	1.52	1.78	1.12	1.49	1.31	1.86	3.03	0.65	0.79	1.14	6.48	1.58	0.74	5.72	4.14	1.87	2.57	1.65	1.01	1.73	2.26	1.50	0.82	0.90	0.84	1.10	1.14	1.04	1.36	1.57	2.82	1.91	1.40	1.58	fipin 1
3.05	3.00	1.53	2.59	2.82	2.20	4.41	4.18	2.25	2.34	4.36	1.68	1.14	1.55	0.80	1.73	1.23	1.31	1.55	2.74	0.96	1.19	2.88	1.01	5.63	4.11	4.31	1.00	0.85	1.34	1.31	1.41	0.79	1.53	1.34	1.07	CD36 antigen
1.74	1.97	1.88	1.81	1.85	1.46	2.31	1.32	2.00	1.90	2.04	1.92	1.08	0.97	1.00	0.97	0.84	1.04	1.39	1.18	1.24	1.13	1.27	1.03	0.85	0.76	0.87	1.40	1.38	1.91	0.83	0.55	1.52	4.96	3.02	3.47	expressed sequence AI315045
45.35	65.24	75.35	51.04	82.18	45.47	1.46	2.77	3.33	0.42	2.54	1.45	1.78	1.42	0.81	1.85	0.30	1.20	1.27	0.93	1.40	0.85	1.69	0.74	0.85	0.88	0.96	1.14	1.02	1.15	1.56	1.41	2.85	0.97	0.79	1.33	farnesyl diphosphate synthetase
3.55	3.08	3.08	3.42	3.52	2.89	1.30	1.11	1.02	0.43	1.00	1.00	0.98	1.13	1.09	0.86	0.31	1.00	1.40	1.10	1.14	0.99	1.07	1.01	2.83	0.93	0.99	1.21	0.16	0.67	7.93	1.94	7.95	0.51	5.39	2.85	cathepsin Z
1.34	1.16	2.16	2.35	1.65	1.86	1.05	0.81	1.54	0.83	1.04	1.33	0.86	0.47	0.88	0.86	1.43	0.64	0.97	0.77	0.94	0.60	0.88	1.43	0.82	1.30	0.24	0.84	1.32	0.83	4.78	6.39	10.62	21.66	32.40	15.54	fatty acid binding protein 4, adipocyte
3.48	2.67	2.42	2.26	2.20	2.67	1.73	1.61	1.30	1.08	1.24	1.08	1.51	1.48	1.25	1.43	0.88	1.16	1.53	1.55	1.25	1.32	1.40	1.17	1.24	1.35	1.32	1.38	1.41	1.54	3.32	3.79	4.25	2.20	2.35	2.83	P450 (cytochrome) oxidoreductase
1.24	1.41	1.15	1.25	1.33	1.17	1.05	1.41	1.24	1.38	1.26	0.99	0.70	0.95	0.93	0.98	0.99	1.12	1.17	1.19	1.23	0.64	1.22	1.18	0.80	1.03	0.90	1.00	0.97	0.97	3.25	4.83	5.97	8.17	8.06	10.09	fatty acid binding protein 1, liver
0.55	0.37	0.31	0.33	0.68	0.56	1.52	0.45	1.39	1.21	1.51	1.13	0.71	0.98	0.83	0.64	1.17	0.57	0.65	0.84	0.84	1.25	0.71	1.45	0.91	0.67	0.73	0.41	1.61	0.93	0.62	0.13	0.14	0.47	0.25	0.14	solute carrier family 24, member 1
0.76	0.48	0.78	0.62	0.48	0.64	0.41	0.84	0.74	0.78	1.28	1.30	0.86	0.89	0.86	0.55	1.61	0.96	0.80	0.99	1.43	1.20	1.16	1.43	0.65	0.61	0.72	0.39	0.91	0.95	0.32	0.36	0.28	1.27	0.87	0.64	cardiac responsive adriamycin protein
1.19	1.48	1.80	1.58	1.55	1.46	1.24	1.52	1.28	1.48	1.67	1.27	0.89	0.89	1.08	0.90	0.79	1.08	0.77	0.98	1.01	1.05	1.10	0.99	0.52	0.46	0.98	0.53	1.41	0.94	0.17	0.37	0.39	2.00	0.90	0.54	RIKEN cDNA 1210007E11 gene

＊　各処理において共通性の高かった遺伝子に関して異種データの相同遺伝子のデータを比較した。

ピンクは発現上昇、水色は発現低下

図7　DEN処理したマウス肝臓の可溶性画分の２次元電気泳動による解析

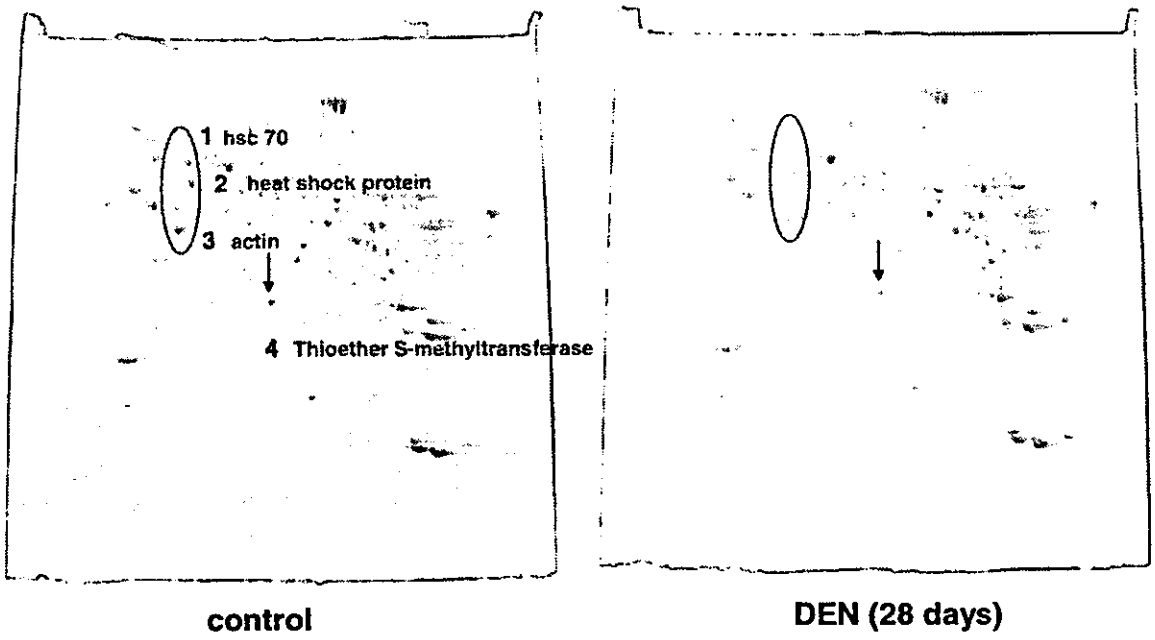

図8　ペプチドマスフィンガープリンティング法によるタンパクの同定例

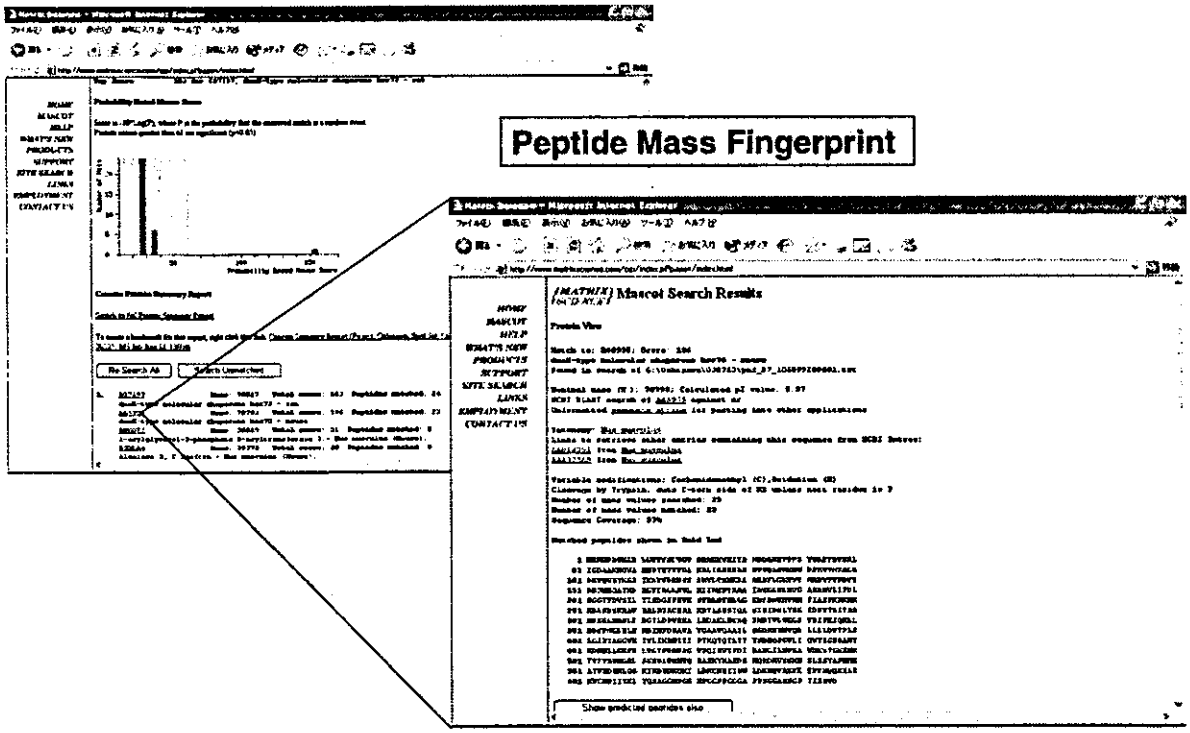

図9　２次元液体クロマトグラムシステム

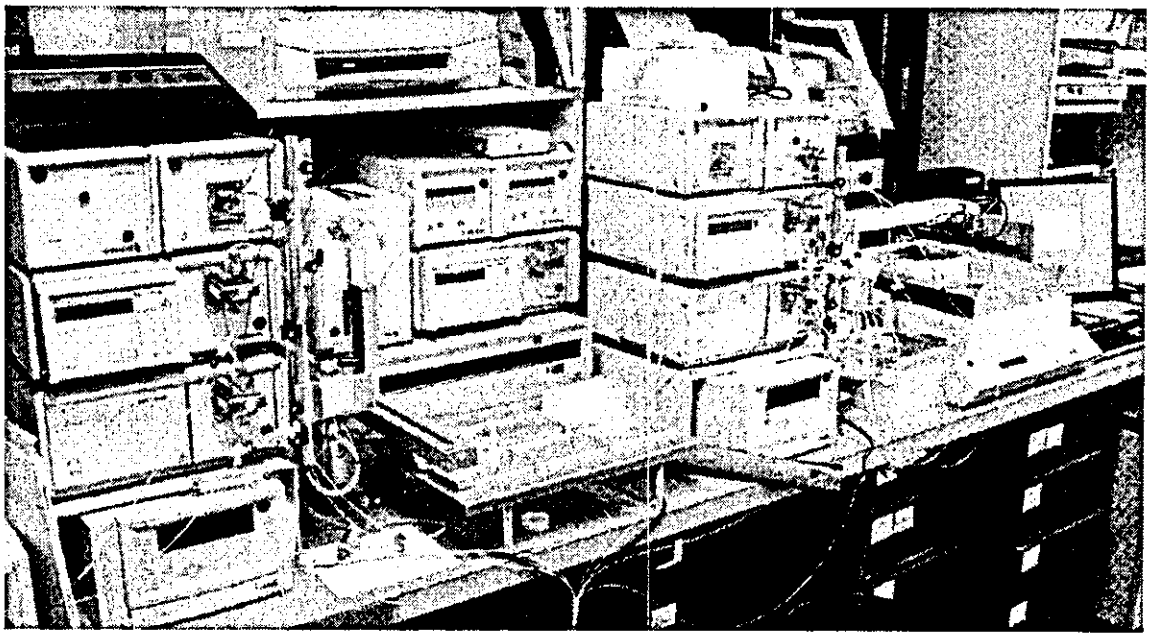

図１０　タンパク質溶液の２次元分離例

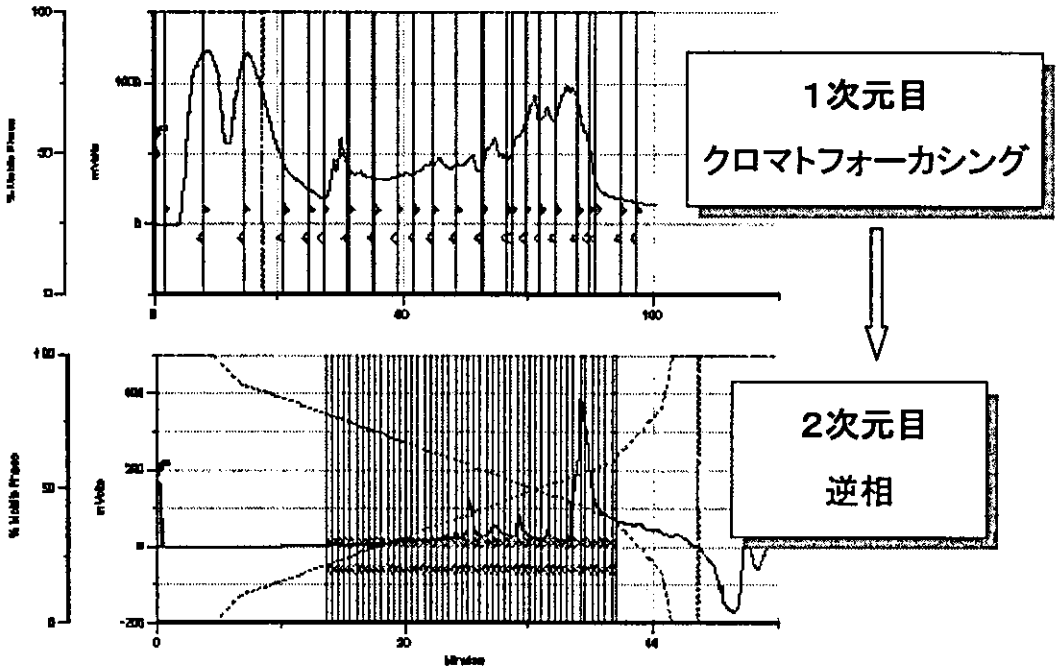

別添4

II. 研究成果の刊行に関する一覧表

平成14年度～16年度

別添4

研究成果の刊行に関する一覧表(平成14年度から16年度)

雑誌

	発表者氏名	論文タイトル名	発表誌名	巻号	ページ	出版年
1)	Takayoshi Suzuki, Yuki Nagano, Akiyasu Kouketsu, Azusa Matsuura, Sakiko Maruyama, Mineko Kurotaki, Hidehiko Nakagawa, Naoki Miyata	Novel inhibitors of human histone deacetylases: design, synthesis, enzyme inhibition, and cancer cell growth inhibition of SAHA-based non- hydroxamates	*J. Med. Chem.*	48	1019-1032	2005
2)	Shinya Usui, Takayoshi Suzuki, Yoshifumi Hattori, Kazuma Etoh, Hiroki Fujieda, Makoto Nishizuka, Masayoshi Imagawa, Hidehiko Nakagawa, Kohfuku Kohda, Naoki Miyata	Design, synthesis and biological activity of novel PPARg ligands based on rosiglitazone and 15d-PGJ2	*Bioorganic & Medicinal Chemistry Letters*	15	1545-1551	2005
3)	Takayoshi Suzuki, Azusa Matsuura, Akiyoshi Kouketsu, Hidehiko Nakagawa, Naoki Miyata	Identification of a potent non-hydroxamate histone deacetylase inhibitor by mechanism-based drug design	*Bioorganic & Medicinal Chemistry Letters*	15	331-335	2005
4)	鈴木孝禎、宮田直樹	ヒストン脱アセチル化酵素阻害剤開発の最前線	*ファルマシア*	41	*in press*	2005
5)	鈴木孝禎、中川秀彦、宮田直樹	癌の分子標的治療薬の開発:非ヒドロキサム酸系ヒストン脱アセチル化酵素阻害薬の設計、合成と生物活性評価	*有機合成化学協会誌*	63	*in press*	2005
6)	Takayoshi Suzuki, Akiyasu Kouketsu, Azusa Matsuura, Arihiro Kohara, Shin-ichi Ninomiya, Kohfuku Kohda, Naoki Miyata	Thiol-based SAHA analogues as potent histone deacetylase inhibitors,	*Bioorganic & Medicinal Chemistry Letters*	14(12)	3313-3317	2004
7)	Masaaki Kurihara, Abu Shara Shamsur Rouf, Hisao Kansui, Hiroyuki Kagechika, Haruhiro Okuda, Naoki Miyata	Design and synthesis of cyclic urea compounds: a pharmacological study for retinoidal acty	*Bioorganic & Medicinal Chemistry Letters*	14(16)	4131-4134	2004
8)	Nobuyuki Sera, Hiroshi Tokiwa, Hideo Utsumi, Shigeki Sasaki, Kiyoshi Fukuhara, Naoki Miyata	Associations between chemical properties and oxidative damage due to nitrophenanthrenes and their related compounds in primary rat hepatocytes	*Polycyclic Aromatic Compounds*	24(4-5)	487-500	2004
9)	I. Nakanishi, K. Ohkubo, K. Miyazaki, W. Hakamata, S. Urano, T, Ozawa, H. Okuda, S, Fukuzumi, N. Ikota, and K. Fukuhara	A planar catechin analogue having a more negative oxidation potential than (+)-catechin as an electron-transfer antioxidant against a peroxyl Rradical	*Chem. Res. Toxicol.*	17	26-31	2004
10)	Yamada K, Suzuki T, Kohara A, Hayashi M, Mizutani T, Saeki K	In vivo mutagenicity of benzo[f]quinoline, benzo[h]quinoline, and 1,7-phenanthroline using the lac Z transgenic mice	*Mutation Research*	559	83-95	2004
11)	Arlt VM, Zhan L, Schmeiser HH, Honma M, Hayashi M, Phillips DH, Suzuki T	DNA adducts and mutagenic specificity of the ubiquitous environmental pollutant 3-nitrobenzanthrone in Muta Mouse	*Environ. Mol. Mutagen.*	43	186-195	2004
12)	Li Zhana, Hiroko Sakamoto, Mayumi Sakuraba, De-Sheng Wu, Li-Shi Zhang, Takayoshi Suzuki, Makoto Hayashi, Masamitsu Honma	Genotoxicity of micro-LR in human lymphoblastoid TK6 cells	*Mutation Research*	557	1-6	2004

	発表者氏名	論文タイトル名	発表誌名	巻号	ページ	出版年
13)	Takayoshi Suzuki, Yuki Nagano, Azusa Matsuura, Arihiro Kohara, Shin-Ichi Ninomiya, Kohfuku Kohda, Naoki Miyata	Novel histone deacetylase inhibitors: design, synthesis, enzyme inhibition, and binding mode study of SAHA-Based non-hydroxamates	*Bioorganic & Medicinal Chemistry Letters*	13(24)	4321-4326	2003
14)	Ken-ichi Saeki, Tomoaki Matsuda, Taka-aki Kato, Katsuya Yamada, Takaharu Mizutani, Saburo Matsui, Kiyoshi Fukuhara, Naoki Miyata	Activation of the Human Ah Receptor by Aza-Polycyclic Aromatic Hydrocarbons and Their Halogenated Derivatives	*Biol. Pharm. Bull.*	26(4)	448-452	2003
15)	Hiroshi Tokiwa, Nobuyuki Sera, Kiyoshi Fukuhara, Hideo Utsumi, Shigeki Sasaki, Naoki Miyata	Structural activity relationship between Salmonella-mutagenicity and nitro-orientation of nitroazaphenanthrenes	*Chemico-Biological Interactions*	146(1)	19-25	2003
16)	Yamada K., Suzuki T., Hakura A., Mizutani T., Saeki K.,	Metabolic activation of 10-aza-substituted benzo[a]pyrene by cytochrome P4501A2 in human liver microsome	*Mutation Research*	557	159-165	2003
17)	Thybaud V., Dean S., Nohmi T., de Boer J., Douglas G. R., Glickman B. W., Gorelick N. J., Heddle J. A., Heflick R. H., Lambert I., Martus H. J., Mirsalis J. C., Suzuki T., Yajima N.	In vivo transgenic mutation	*Mutation Research*	540	141-151	2003
18)	Itoh T., Kuwahara T., Suzuki T., Hayashi M., Ohnishi Y.	Regional mutagenicity of Heteroocyclic amines in the intestine: mutation analysis of the *cII* gene in lambda/lacZ transgenic mice	*Mutation Research*	539	99-108	2003
19)	Ikuo Nakanishi, Shunichi Fukuzumi, Toshifumi Konishi, kei Ohkubo, Mamoru Fujitsuka, Osamu Ito and Naoki Miyata	DNA Cleavage via Superoxide Anion Formed in Photoinduced Electron Transfer from NADH to gamma-Cyclodextrin-Bicapped C60 in an Oxygen-Saturated Aqueous Solituion	*J. Phys. Chem. B*	106(9)	2372-2380	2002
20)	Kiyoshi Fukuhara, Ikuo Nakanishi, Hisao Kansui, Etsuko Sugiyama, Mitsuhiro Kimura, Tomokazu Shimada, Shiro Urano, Kentaro Yamaguchi, and Naoki Miyata	Enhanced Radical-Scavenging Activity of a Planar Catechin Analogue	*J. Am. Chem. Soc.*	124(21)	5952-5953	2002
21)	Matsuoka, Atsuko; Takeshita, Kenji; Furuta, Ayumi; Ozaki, Masayasu; Fukuhara, Kiyoshi; Miyata, Naoki	The 4'-hydroxy group is responsible for the in vitro cytogenetic activity of resveratrol	*Mutation Research*	521(1-2)	29-35	2002
22)	Yamada K, Suzuki T, Kohara A, Hayashi M, Hakura A, Mizutani T, Saeki K.	Effect of 10-aza-substitution on benzo[a]pyrene mutagenicity in vivo and in vitro.	*Mutation Research*	521	187-200	2002
23)	Kohara A, Suzuki T, Honma M, Ohwada T, Hayashi M	Dinitropyrenes induce gene mutations in multiple organs of the lambda/lacZ transgenic mouse (Muta Mouse)	*Mutation Research*	515	73-83	2002
24)	Kohara A, Suzuki T, Honma M, Ohwada T, Hayashi M.	Mutagenicity of aristolochic acid in the lambda/lacZ transgenic mouse (MutaMouse)	*Mutation Research*	515	63-72	2002

III. 研究成果の刊行物・別刷

平成14年度～平成16年度

Novel Inhibitors of Human Histone Deacetylases: Design, Synthesis, Enzyme Inhibition, and Cancer Cell Growth Inhibition of SAHA-Based Non-hydroxamates

Takayoshi Suzuki,*,† Yuki Nagano,† Akiyasu Kouketsu,† Azusa Matsuura,† Sakiko Maruyama,‡ Mineko Kurotaki,‡ Hidehiko Nakagawa,† and Naoki Miyata*,†

Graduate School of Pharmaceutical Sciences, Nagoya City University, 3-1 Tanabe-dori, Mizuho-ku, Nagoya, Aichi 467-8603, Japan, and Evaluation Group, Drug Research Department, R. & D. Division, Pharmaceuticals Group, Nippon Kayaku Co., Ltd., 31-12, Shimo 3-chome, Kita-ku, Tokyo 115-8588, Japan

Received October 1, 2004

To find novel non-hydroxamate histone deacetylase (HDAC) inhibitors, a series of compounds modeled after suberoylanilide hydroxamic acid (SAHA) was designed and synthesized. In this series, compound **7**, in which the hydroxamic acid of SAHA is replaced by a thiol, was found to be as potent as SAHA, and optimization of this series led to the identification of HDAC inhibitors more potent than SAHA. In cancer cell growth inhibition assay, *S*-isobutyryl derivative **51** showed strong activity, and its potency was comparable to that of SAHA. The cancer cell growth inhibitory activity was verified to be the result of histone hyperacetylation and subsequent induction of $p21^{WAF1/CIP1}$ by Western blot analysis. Kinetical enzyme assay and molecular modeling suggest the thiol formed by enzymatic hydrolysis within the cell interacts with the zinc ion in the active site of HDACs.

Introduction

The reversible acetylation of the ϵ-amino groups of specific histone lysine residues by histone deacetylases (HDACs) and histone acetyl transferases is an important regulatory mechanism of gene expression.[1] When HDACs are inhibited, histone hyperacetylation occurs. The disruption of the chromatin structure by histone hyperacetylation leads to the transcriptional activation of a number of genes.[2] One important outcome of the activation is induction of the cyclin-dependent kinase inhibitory protein $p21^{WAF1/CIP1}$, which causes cell cycle arrest.[3] Indeed, HDAC inhibitors such as trichostatin A (TSA) and suberoylanilide hydroxamic acid (SAHA) (Chart 1) have been reported to inhibit cell growth, induce terminal differentiation in tumor cells,[4] and prevent the formation of malignant tumors in mice.[5] Therefore, HDACs have emerged as attractive targets in anticancer drug development, and HDAC inhibitors have also been viewed as useful tools to study the function of these enzymes.

Many groups have ongoing research programs to find nonpeptide small-molecule inhibitors of HDACs, and these efforts have led to the identification of several classes of inhibitors.[6] Most previously reported HDAC inhibitors belong to hydroxamic acid derivatives, typified by TSA and SAHA, which are thought to chelate the zinc ion in the active site in a bidentate fashion through its CO and OH groups.[7] However, hydroxamic acids occasionally have been associated with problems such as poor pharmacokinetics and severe toxicity.[8] Thus, it has become increasingly desirable to find

Chart 1

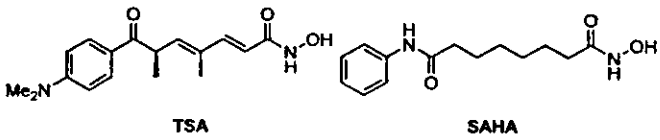

replacements that possess strong inhibitory action against HDACs. In addition, in terms of biological research, the discovery of novel zinc-binding groups (ZBGs) may lead to a new type of HDAC isozyme-selective inhibitors which are useful as tools for probing the biology of the enzyme.[9] Thus far, *o*-aminoanilide,[9,10] electrophilic ketones,[11] and *N*-formyl hydroxylamine[12] have been reported as ZBGs in small-molecule HDAC inhibitors. However, most of them have reduced potency as compared to hydroxamic acid, and unfortunately, HDAC inhibitors bearing electrophilic ketones[11] have a metabolic disadvantage in that they are readily reduced to inactive alcohols in vivo, even within cells. We therefore initiated a search for replacement groups for hydroxamic acid with the goal of drug discovery as well as finding new tools for biological research, and found some potent non-hydroxamate small-molecule HDAC inhibitors.[13] We now present a full account of our study reporting the design, synthesis, HDAC inhibition, cancer cell growth inhibition, and binding mode analysis of non-hydroxamates based on the structure of SAHA.

Chemistry

The compounds prepared for this study are shown in Tables 1−5. The routes used for synthesis of the compounds are shown in Schemes 1−4. Scheme 1 shows the preparation of compounds **4**, **5**, **10**, **12**−**17**, and **18**. Compounds **4** and **5** were synthesized from pimelic acid **56**. The condensation of pimelic acid **56** with an equiva-

* To whom correspondence should be addressed. Tel and fax: +81−52−836−3407; e-mail: miyata-n@phar.nagoya-cu.ac.jp; suzuki@phar.nagoya-cu.ac.jp

† Graduate School of Pharmaceutical Sciences, Nagoya City University.

‡ Nippon Kayaku Co., Ltd.

10.1021/jm049207j CCC: $30.25
Published on Web 01/25/2005

Scheme 1[a]

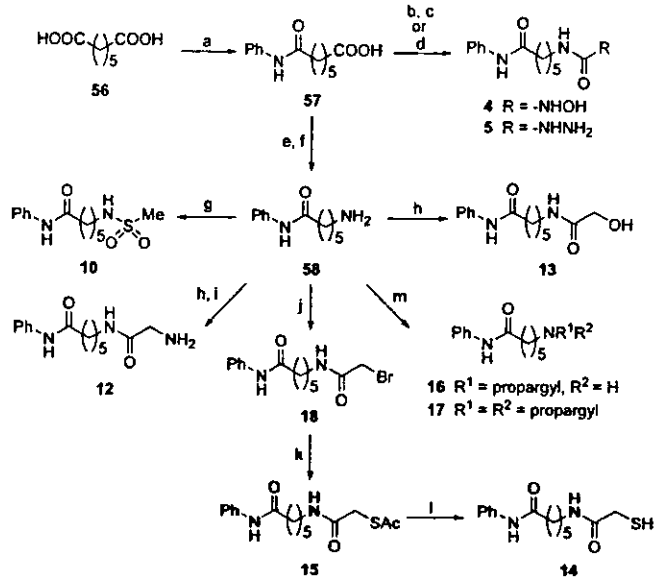

[a] Reagents and conditions: (a) aniline, 180 °C; (b) diphenylphosphoryl azide (DPPA), Et_3N, toluene, reflux, and then *O*-(2-tetrahydropyranyl)hydroxylamine, reflux; (c) TsOH, MeOH, rt; (d) DPPA, Et_3N, benzene, reflux, and then hydrazine monohydrate, reflux; (e) DPPA, Et_3N, benzene, reflux, and then BnOH, reflux; (f) H_2, 5%Pd–C, MeOH, rt; (g) MsCl, pyridine, rt; (h) $HOCH_2COOH$ or $BocNHCH_2COOH$, EDCI, HOBt, DMF, rt; (i) TFA, $CHCl_3$, rt; (j) $BrCH_2COBr$, Et_3N, THF, rt; (k) AcSK, EtOH, rt; (l) K_2CO_3, MeOH, rt; (m) propargyl bromide, K_2CO_3, MeOH, rt.

lent amount of aniline gave mono-anilide **57**. Curtius rearrangement of the acyl azide prepared from carboxylic acid **57** using diphenylphosphoryl azide provided the isocanates, which on treatment with *O*-tetrahydropyranyl (THP) hydroxylamine or hydrazine gave *O*-THP hydroxyurea and semicarbazide **5**. Deprotection of the THP group of the *O*-THP hydroxyurea under acidic conditions afforded hydroxyurea **4**.

Compounds **10**, **12**–**17**, and **18** were prepared from carboxylic acid **57** obtained above via amine **58** by the procedure outlined in Scheme 1. Carboxylic acid **57** was converted to amine **58** with a three-step sequence: Curtius rearrangement of the acyl azide prepared from carboxylic acid **57**, treatment of the resulting isocyanates with benzyl alcohol, and removal of the Z group by hydrogenation. Coupling between amine **58** and methanesulfonyl chloride afforded sulfonamide **10**. The reaction of amine **58** with *N*-Boc glycine in the presence of EDCI and HOBt in DMF was followed by treatment with trifluoroacetic acid to give aminoacetamide **12**. Hydroxyacetamide **13** was obtained in one step using the procedure described for **12**. The amino group of **58** was acylated with bromoacetyl bromide to yield bromoacetamide **18**. Bromide **18** was treated with potassium thioacetate to give thioacetate **15**, after which deacetylation of the thioacetate in the presence of K_2CO_3 in MeOH gave mercaptoacetamide **14**. The amine **58** was allowed to react with propargyl bromide in the presence of K_2CO_3 to give mono- and di-alkylated compounds **16** and **17**.

Compounds **6**–**9**, **11**, **19**–**21**, **24**–**32**, and **37** were prepared from another starting material, **59** (Scheme 2). The preparation of hydroxysulfonamide **6** was achieved via sulfonyl chloride **60**. Bromide **59** was converted to sulfonyl chloride **60** by sulfation and by a

Scheme 2[a]

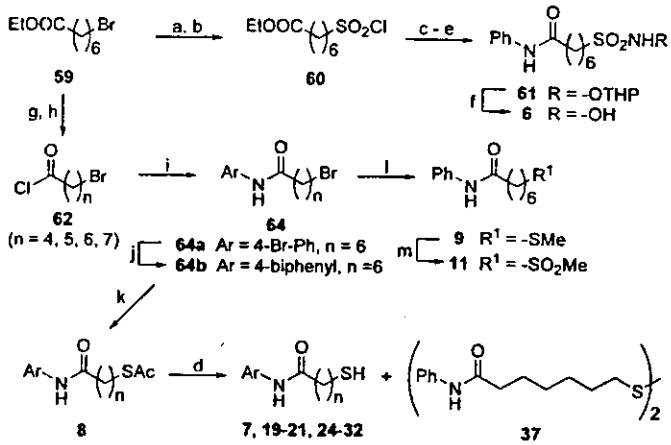

[a] Reagents and conditions: (a) Na_2SO_3, EtOH, H_2O, reflux; (b) $SOCl_2$, DMF, toluene, reflux; (c) *O*-(2-tetrahydropyranyl)hydroxylamine, 4-(dimethylamino)pyridine, pyridine, CH_2Cl_2, rt; (d) 2N aq NaOH, EtOH, rt; (e) aniline, EDCI, HOBt, DMF, rt; (f) TFA, CH_2Cl_2, 60 °C; (g) $LiOH{\cdot}H_2O$, EtOH, THF, H_2O, rt; (h) $(COCl)_2$, DMF, CH_2Cl_2, rt; (i) $ArNH_2$ (**63**), Et_3N, CH_2Cl_2, rt; (j) $PhB(OH)_2$, $Pd(PPh_3)_4$, $NaHCO_3$, 1-methyl-2-pyrrolidinone, H_2O, 80 °C; (k) AcSK, EtOH, rt; (l) 15% aq NaSMe, EtOH, rt; (m) *m*-chloroperoxybenzoic acid, CH_2Cl_2, rt.

subsequent reaction with thionyl chloride. The sulfonyl chloride **60** was treated with *O*-THP hydroxylamine to give *O*-THP hydroxysulfonamide, after which hydrolysis of the ester under alkaline conditions and subsequent amide formation with aniline gave compound **61**. Removal of the THP group of compound **61** by treatment with trifluoroacetic acid gave hydroxysulfonamide **6**.

Compounds **7**–**9**, **11**, **19**–**21**, **24**–**32**, and **37** were synthesized from the corresponding acid chlorides **62** (**62a** ($n = 4$) and **62b** ($n = 5$) are commercially available) by the route shown in Scheme 2. **62c** ($n = 6$) was prepared from ester **59** by hydrolysis of the ethyl ester and a subsequent reaction with oxalyl chloride, and **62d** ($n = 7$) was obtained in the same way as **62c**. The amino group of aromatic amines **63** was acylated with an appropriate acid chloride **62** to give the amides **64**. Suzuki coupling[14] of bromobenzene **64a** with phenylboronic acid provided the biphenyl **64b**. Bromides **64** were treated with potassium thioacetate to give compound **8**, after which hydrolysis of the thioacetates under alkaline conditions gave the desired compounds **7**, **19**–**21**, **24**–**31**, and **32**, and disulfide **37** was obtained as a byproduct when thiol **7** was synthesized. Sulfide **9** was prepared by the alkylation of methylmercaptan with bromide **64c** (Ar = Ph, $n = 6$). Oxidation of **9** with 2 equiv of *m*-chloroperoxybenzoic acid provided the sulfone **11**.

Thiols **22**, **23**, **33**–**35**, and **36** were prepared from alcohol **65** or **66** by the procedure outlined in Scheme 3. Treatment of bromide **65** with phenol in the presence of K_2CO_3 gave ether **67**, and condensation of amine **66** with an appropriate aromatic carboxylic acid **69** afforded amides **68**. Alcohols **67** and **68** were converted to thiols **22**, **23**, **33**–**35**, and **36** in three steps by conversion of the alcohols to bromides, treatment of the bromides with potassium thioacetate, and hydrolysis of the resulting thioacetates.

The preparation of *S*-chemically modified compounds **38**–**54**, and **55** is shown in Scheme 4. Thiols **7**, **26**, **28**–**32**, **34**, **35**, and **36** were coupled with the corresponding

Scheme 3[a]

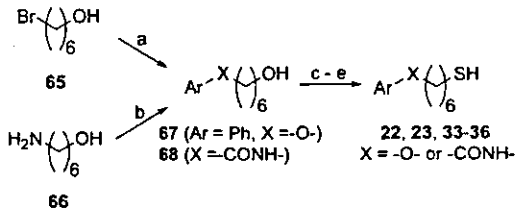

[a] Reagents and conditions: (a) Phenol, K_2CO_3, DMF, 80 °C; (b) ArCOOH (**69**), EDCI, HOBt, DMF, rt; (c) CBr_4, PPh_3, CH_2Cl_2, 0 °C; (d) AcSK, EtOH, rt; (e) 2N aq NaOH, EtOH, THF, rt.

Scheme 4[a]

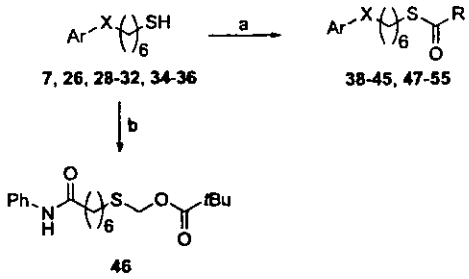

[a] Reagents and conditions: (a) RCOCl (**70**), 4-(dimethylamino)pyridine, pyridine, CH_2Cl_2, rt; (b) NaH, chloromethyl pivalate, DMF, 0 °C to room temperature.

acyl chloride **70** to give thioesters **38–45**, **47–54**, and **55**. Alkylation of thiol **7** with chloromethyl pivalate in the presence of sodium hydride in DMF afforded compound **46**.

Results and Discussion

Enzyme Assays. The compounds synthesized in this study were tested with an in vitro assay using a HeLa nuclear extract rich in HDAC activity. The results are summarized in Tables 1–3.

The IC_{50} values of SAHA and *o*-aminoanilide **1** were 0.28 μM and 120 μM, respectively (entries 1 and 2). α-Ketoamide **2** and *N*-formyl hydroxylamine **3** were reported previously to inhibit HDACs with an IC_{50} of 0.34 μM and 2.8 μM, respectively (entries 3 and 4).[11b,12]

The crystal structures of an archaebacterial HDAC homologue (HDAC-like protein, HDLP)/hydroxamates and HDAC8/hydroxamates complexes made it clear that the hydroxamic acid group coordinates the zinc ion in the active site through its CO and OH groups and also forms three hydrogen bonds between its CO, NH, and OH groups and Tyr 306, His 143, and His 142 (HDAC8 numbering), respectively.[7] From these data, hydroxyurea **4**, semicarbazide **5**, and hydroxysulfonamide **6** were synthesized and tested as HDAC inhibitors because it is possible for them to chelate zinc ion and form hydrogen bonds with Tyr and His like SAHA. Among these three compounds, hydroxyurea **4** and semicarbazide **5** showed anti-HDAC activity and the IC_{50} values were comparable to that of *o*-aminoanilide **1** (entries 5, 6, and 7). However, they were much less effective than SAHA.

Thiols seemed to be reasonable targets for hydroxamic acid replacements, because zinc ion is highly thiophilic and thiol derivatives have been reported to inhibit zinc-dependent enzymes such as angiotensin converting enzyme[15] and matrix metalloproteinases.[16] Furthermore, macrocyclic compounds bearing a disulfide group such as FK228 have been reported recently to inhibit

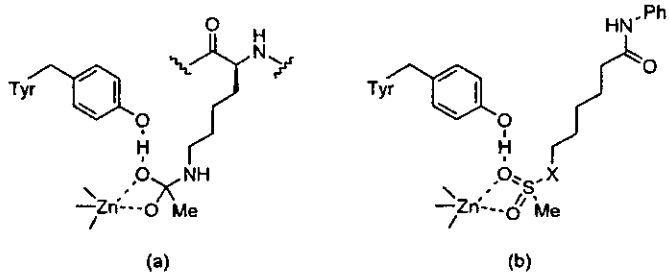

Figure 1. The transition state proposed for HDACs (a), and models for the binding of sulfone derivatives (b).

HDACs under reductive conditions.[17] Surprisingly, although the inhibitory ability of monodentate ZBGs such as thiol was thought to be less than that of bidentate ZBGs such as hydroxamate, *N*-formyl hydroxylamine, and hydrated electrophilic ketones,[16] the activity of thiol **7** was far greater than expected. A pronounced inhibitory effect (IC_{50} = 0.21 μM) was observed with thiol **7**, which was much more active than previously reported non-hydroxamates such as *o*-aminoanilide, *N*-formyl hydroxylamine, and trifluoromethyl ketone,[11a] and as potent as α-ketoamide **2** and SAHA (entry 8). To confirm that the thiol group plays an important role in anti-HDAC activity, thioacetate **8a** and methyl sulfide **9** were tested. As expected, thiol transformation into thioacetate and methyl sulfide led to an inhibitor that was about 30-fold less potent and a compound devoid of anti-HDAC activity, respectively (entries 9 and 10). These results suggest that thiolate anion generated under physiological conditions has an intimate involvement in the interaction with the zinc ion in the active site.

The crystal structures of the HDLP/hydroxamates and HDAC8/hydroxamates complexes have led to a solid understanding of not only the three-dimensional structure of the active site of HDACs but also the catalytic mechanism for the deacetylation of acetylated lysine substrate.[7] It has been proposed that the carbonyl oxygen of this substrate could bind the zinc, and the carbonyl could be attacked by a zinc-chelating water molecule (Figure 2a), which would result in the production of deacetylated lysine via a tetrahedral carbon-containing transition state (Figure 1a). On the basis of the proposed catalytic mechanism, we attempted to design non-hydroxamate HDAC inhibitors. First, we designed transition-state (TS) analogues. The TS of HDAC deacetylation was estimated to include a tetrahedral carbon (Figure 1a) as with other zinc proteases.[18] We focused attention on sulfone derivative TS analogues because it has been suggested that the sulfonamide moiety has strong similarity with the TS of amide bond hydrolysis, both from a steric and an electronic point of view.[19] Compounds **10** and **11**, in which a hydroxamic acid of SAHA is replaced by a sulfonamide and a sulfone, respectively, were designed and synthesized as TS analogues (Figure 1b). Of these two TS analogues, sulfone **11** showed anti-HDAC activity and the IC_{50} value was 230 μM (entries 11 and 12). However, sulfone **11** was approximately 820-fold less effective than SAHA.

Our next approach was based on the proposed deacetylation mechanism whereby a zinc-chelating water molecule activated by His142 and His 143 (HDAC8 numbering) makes a nucleophilic attack on the carbonyl carbon of an acetylated lysine substrate (Figure 2a).

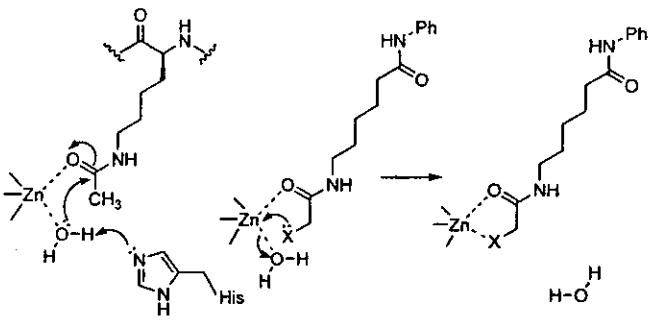

Figure 2. The mechanism proposed for the deacetylation of acetylated lysine substrate (a), and a model for the binding of heteroatom-containing substrate analogues to zinc ion (b).

Table 1. HDAC Inhibition Data for SAHA and SAHA-based Non-hydroxamtes[a]

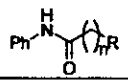

entry	compd	R	*n*	% inhbtn at 100 μM	IC_{50} (μM)
1	SAHA[b]	-CONHOH	6	100	0.28
2	1[c]	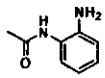	6	48	120
3	2	-COCONHMe	6	ND	0.34[d]
4	3		7	ND	2.8[e]
5	4	-NHCONHOH	5	58	80
6	5	-NHCONHNH$_2$	5	35	150
7	6	-SO$_2$NHOH	6	14	>100
8	7	-SH	6	100	0.21
9	8a	-SAc	6	85	7.1
10	9	-SMe	6	11	>100
11	10	-NHSO$_2$Me	5	10	7500
12	11	-SO$_2$Me	6	33	230
13	12[f]	-NHCOCH$_2$NH$_2$	5	6	>100
14	13	-NHCOCH$_2$OH	5	0	>100
15	14	-NHCOCH$_2$SH	5	99	0.39
16	15	-NHCOCH$_2$SAc	5	72	22
17	16		5	14	>100
18	17		5	0	>100
19	18	-NHCOCH$_2$Br	5	78	17

[a] Values are means of at least three experiments. [b] Prepared as described in ref 26. [c] Prepared as described in ref 9a. [d] Data taken from the literature (ref 11b). [e] Data taken from the literature (ref 12). [f] Trifluoroacetic acid salt. ND = No data.

Table 2. Effect of Linker Variation on HDAC Inhibitory Activity of Thiols[a]

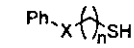

entry	compd	X	*n*	IC_{50} (μM)
1	7	-NHCO-	6	0.21
2	19	-NHCO-	7	1.5
3	20	-NHCO-	5	0.37
4	21	-NHCO-	4	6.2
5	22	-O-	6	11
6	23	-CONH-	6	0.36

[a] Values are means of at least three experiments.

Table 3. Effect of Aromatic Group Variation on HDAC Inhibitory Activity of Thiols[a]

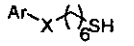

entry	compd	Ar	X	IC_{50} (μM)
1	7	-Ph	-NHCO-	0.21
2	24		-NHCO-	1.2
3	25		-NHCO-	1.1
4	26		-NHCO-	0.075
5	27		-NHCO-	0.62
6	28		-NHCO-	0.21
7	29		-NHCO-	0.11
8	30		-NHCO-	0.072
9	31		-NHCO-	0.17
10	32		-NHCO-	0.34
11	23	-Ph	-CONH-	0.36
12	33		-CONH-	0.61
13	34		-CONH-	0.085
14	35		-CONH-	0.079
15	36		-CONH-	0.10

[a] Values are means of at least three experiments.

With this mechanism, if the water molecule is forcibly removed from the zinc ion, the HDACs would supposedly be inhibited. We then designed and synthesized heteroatom-containing substrate analogues **12**, **13**, and **14**. These analogues would be recognized as substrates by HDACs and would be easily taken into the active site where they could force the water molecule off the zinc ion and the reactive site for the deacetylation by chelation of the heteroatom to the zinc ion, and might behave as HDAC inhibitors (Figure 2b). As shown in Table 1 (entries 13, 14, and 15), potent inhibition was observed with mercaptoacetamide **14**, while **12** and **13** did not possess HDAC inhibitory activities. Mercaptoacetamide **14** exhibited an IC_{50} of 0.39 μM, and its activity largely surpassed those of *o*-aminoanilide **1** and *N*-formyl hydroxylamine **3** and was comparable to those of α-ketoamide **2** and SAHA. As expected, thiol transformation into thioacetate (**15**) led to a 55-fold less potent inhibitor. This result suggests the ease of ionization of thiol is an important factor for HDAC inhibition like the case of thiol **7**.

We turned our attention to irreversible HDAC inhibitors. TPX B is an irreversible HDAC inhibitor,[20] and finding more specific and simpler irreversible HDAC inhibitors is useful for the isolation and cloning of an HDAC.[2] As described above, the crystal structures of the HDLP/hydroxamates and HDAC8/hydroxamates complexes revealed that the hydroxamic acid group forms three hydrogen bonds with Tyr 306, His 143, and His 142, and furthermore, zinc ion is coordinated by His 180, Asp 178, and Asp 267 (HDAC8 numbering). Since the phenol group of Tyr, the imidazole group of His, and the carboxyl group of Asp are able to react with electrophiles, we prepared analogues bearing propargyl

Table 4. Cell Growth Inhibition Data on NCI-H460 Cells for Compound **7** and Its *S*-Modified Prodrugs[a]

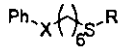

entry	compd	R	EC_{50} (μM)
1	7	-H	>50[b]
2	37	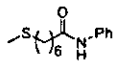	>50[c]
3	38	-Ac	36
4	39	-COEt	28
5	40	-CO*n*-Pr	22
6	41	-CO*i*-Pr	20
7	42	-CO*t*-Bu	>50[d]
8	43		27
9	44		21
10	45	-Bz	25
11	46	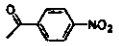	24
12		$-CH_2OCO$*t*-Bu	25

[a] Values are means of at least two experiments. [b] 34% inhibition at 50 μM. [c] 10% inhibition at 50 μM. [d] 42% inhibition at 50 μM.

amino (**16**, **17**) and bromoacetamide (**18**) which could form covalent bonds with Tyr, His, and Asp of the enzyme, and evaluated their anti-HDAC activities. While propargyl amino compounds **16** and **17** did not possess HDAC inhibitory activities, more potent inhibition was observed with bromoacetamide **18** (entries 17, 18, and 19). Bromoacetamide **18** exhibited an IC_{50} of 17 μM and its activity was about 9-fold as strong as that of *o*-aminoanilide **1**, but much weaker than that of SAHA.

With the results shown in Table 1, we were encouraged to study further the structure–activity relationship (SAR) and structural optimization. We selected thiol **7** for further study.[21] First, we examined the effect of linker parts of thiol **7**. The results are summarized in Table 2. HDAC inhibition was distinctly dependent on chain length, with $n = 7$ (**19**) and $n = 4$ (**21**) resulting in less potent inhibitors. However, compound **20**, in which $n = 5$, showed essentially the same potency as compound **7**, in which $n = 6$ (entries 1–4). The similar SAR between thiols and hydroxamates, with $n = 6$ optimal,[22] indicates that thiols inhibit HDACs in a binding mode similar to that of hydroxamates. As for the group attaching the phenyl moiety, ether **22** displayed moderate activity, whereas the activity of the reversed amide **23** was maintained (entries 5 and 6).

Next, the aromatic group was examined (Table 3). In the amide-linked series (entries 1–10), 4-substituted phenyl compounds tended to decrease the potency. Specifically, compounds **24** (Ar = 4-NMe_2-Ph), **25** (Ar = 4-biphenyl), and **27** (Ar = 4-PhO-Ph) showed about a 3- to 6-fold decrease in potency when compared to the parent thiol **7** (entries 2, 3, and 5). On the other hand, compound **26**, in which a phenyl group was introduced at the 3-position of the phenyl group of **7**, showed 3-fold increased inhibitory activity (IC_{50} of 0.075 μM, entry 4). In addition, 3-phenoxy compound **28** was equipotent with compound **7** (entry 6). We investigated the effect of the replacement of the phenyl group of compound **7** with heteroaryl rings (entries 7, 8, 9, and 10). Changing the benzene ring to a 3-pyridine ring (**29**), 4-phenyl-2-thiazole ring (**31**), and 2-benzothiazole ring (**32**) sustained or slightly reduced the activity, whereas quinoline **30** had improved activity (IC_{50} of 0.072 μM), and turned out to be the most potent compound in this series. The reverse amide-linked series (entries 11–15) exhibited potencies similar to or greater than the parent thiol **23**, with the exception of **33** (Ar = 4-NMe_2-Ph), which resulted in a slightly less potent inhibitor. In particular, the reversed amides **34** with a naphthalene substituent and **35** with a benzofuran substituent exhibited about 3-fold increases in potency (IC_{50}s of 0.085 μM and 0.079 μM, respectively). As a result, IC_{50}s in the double-digit nanomolar range were observed with 3-biphenyl **26**, quinoline **30**, naphthalene **34**, and benzofuran **35**, which were approximately 3- to 4-fold more potent than SAHA.

Table 5. Cell Growth Inhibition Data on NCI-H460 Cells for Compound **40** and Its Derivatives[a]

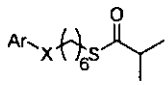

entry	compd	Ar	X	EC_{50} (μM)
1	40	-Ph	-NHCO-	20
2	47		-NHCO-	2.8
3	48		-NHCO-	25
4	49		-NHCO-	2.9
5	50	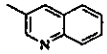	-NHCO-	8.0
6	51	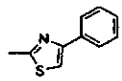	-NHCO-	2.1
7	52	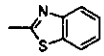	-NHCO-	9.5
8	53	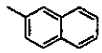	-CONH-	12
9	54	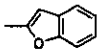	-CONH-	4.1
10	55	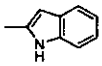	-CONH-	12

[a] Values are means of at least two experiments.

Table 6. Growth Inhibition of Various Cancer Cells Using SAHA and Compound **51**[a]

	cell	SAHA, EC_{50} (μM)	**51**, EC_{50} (μM)
MDA-MB-231	breast cancer	1.5	2.3
SNB-78	central nervous system	16	9.1
HCT116	colon cancer	0.58	3.0
NCI–H226	lung cancer	2.6	2.6
LOX-IMVI	melanoma	1.3	1.1
SK-OV-3	ovarian cancer	2.5	4.5
RXF-631L	renal cancer	2.0	2.4
St-4	stomach cancer	5.2	5.0
DU-145	prostate cancer	1.6	4.5
	mean	3.7	3.8

[a] Values are means of at least two experiments.

Cancer Cell Growth Inhibition Assay. To confirm the effectiveness of thiol-based HDAC inhibitors as anticancer drugs and tools for biological research, thiol **7** was initially tested in a cancer cell growth inhibition

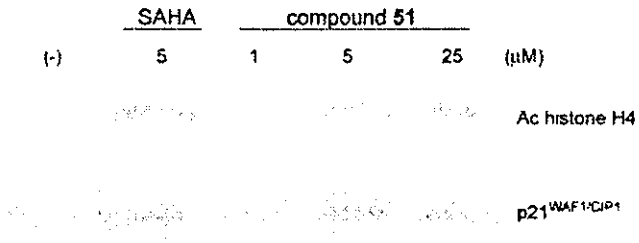

Figure 3. Western blot analysis of histone hyperacetylation and $p21^{WAF1/CIP1}$ induction in HCT 116 cells produced by compound **51** and by reference compound SAHA.

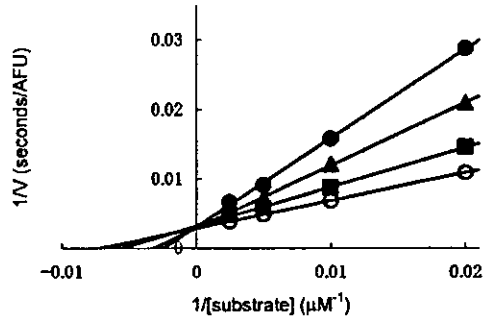

Figure 4. Reciprocal rate vs reciprocal acetylated lysine substrate concentration in the presence of 0.3 (●), 0.1 (▲), 0.03 (■), and 0 (○) μM of **7**.

assay using human lung cancer NCI-H460 cells against which it was found to be only weakly potent, although **7** was highly active in an enzymatic assay (Table 4, entry 1). The reason for the weak activity of thiol **7** is unclear, but it is reasonable to assume that it was due to poor membrane permeability resulting from the highly polar character of this compound, and that a transient masking of the sulfhydryl group could improve its permeability and its ability to inhibit cancer cell growth. Therefore, we investigated the possibility of improving the inhibition using the prodrug approach. In the search for a suitable prodrug of thiols, disulfides seemed to be attractive targets, because it has been reported that the disulfide bond of macrocyclic compounds bearing a disulfide group such as FK228 is reduced in the cellular environment, releasing the free thiol analogue as the active species.[17] However, contrary to our expectation, disulfide **37** failed to exhibit a growth inhibitory effect on NCI-H460 cells (entry 2). Next, we examined the activity of acetyl compound **8a**. Acetyl compound **8a** proved to be relatively potent compared with thiol **7** and disulfide **37** (EC_{50} of 36 μM) (entry 3). This result suggests that **8a** permeates the cell membrane more efficiently than thiol **7**, and is converted to thiol **7** by enzymatic hydrolysis within the cell.[23] Encouraged by this finding, we prepared other *S*-acyl compounds (**38**–**45**) and evaluated their activities (entries 4–11). This series of compounds exhibited greater potency than acetyl compound **8a**, except for pivaloyl compound **41**, which was a less potent inhibitor. In particular, isobutyryl compound **40** showed about a 2-fold increase in activity when compared to acetyl compound **8a** (EC_{50} of 20 μM). The compound bearing a (pivaloyloxy)methyl group[24] (**46**) was slightly less active than isobutyryl compound **40** (entry 12).

With the results shown in Table 4, a selected set of active compounds from the enzymatic assay was *S*-isobutyrylated and tested as cancer cell growth inhibitors (Table 5). Much to our satisfaction, changing the phenyl group of compound **40** to other aromatic groups led to positive results. Isobutyryl analogues **47**–**55** were generally more potent than the parent compound **40**; the sole exception is **48** (Ar = 3-OPh-Ph) which was slightly less active than compound **40** (entry 3). Notably, 3-biphenyl (**47**), 3-pyridinyl (**49**), and 4-phenyl-2-thiazolyl (**51**) analogues showed strong activity in inhibiting the growth of NCI-H460 cells, with EC_{50}s of 2–3 μM. Furthermore, we evaluated cancer cell growth inhibition by SAHA and **51**, the most potent compound in this study, against nine other human cancer cell lines

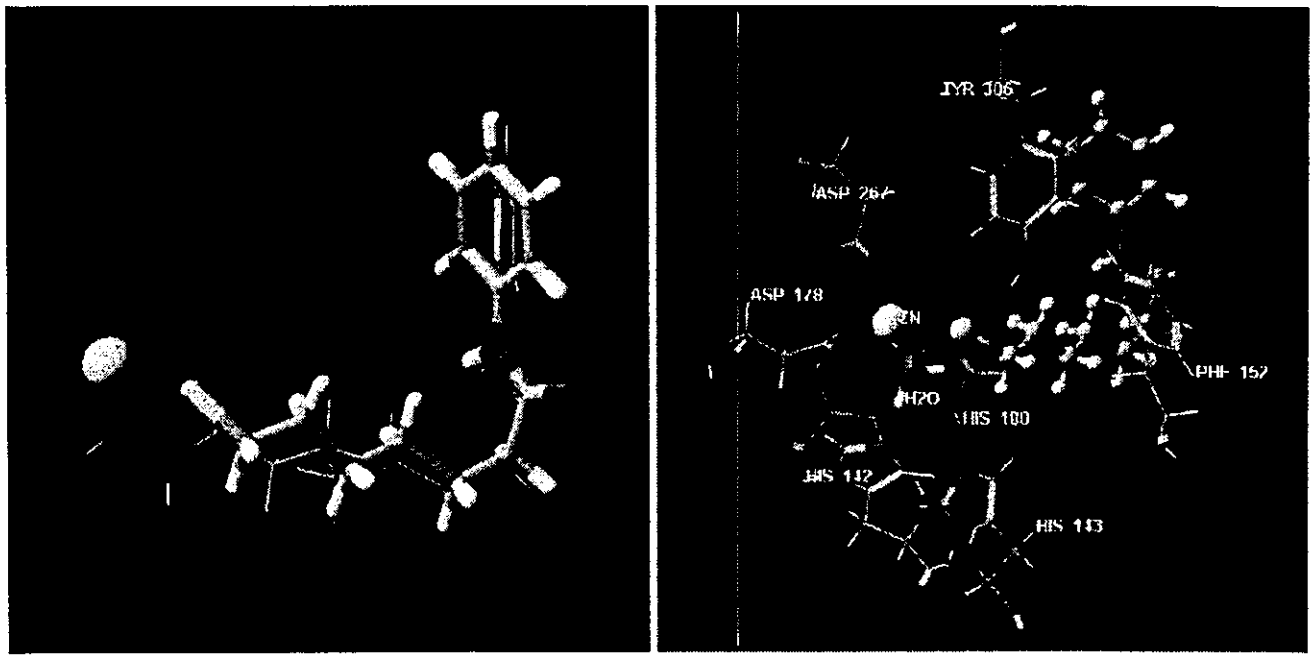

Figure 5. Superposition of the low energy conformations of **7** (tube) and SAHA (wire) (left). The HDAC8 pocket is not shown for the sake of clarity. View of the conformation of **7** (ball-and-stick) docked in the HDAC8 catalytic core (right). Residues around the zinc ion and a water molecule are displayed as wires and tubes, respectively.

(Table 6). Compound **51** exerted potent growth inhibition against various human cancer cells, with EC_{50} values ranging from 1 to 10 μM, and these inhibitory activities were comparable to those of SAHA (average EC_{50} of **51** 3.8 μM, SAHA 3.7 μM) which is currently being evaluated in clinical trials for use in the treatment of cancer.

By Western blot analysis, cancer cell growth inhibition with compound **51** was verified to be the result of inhibition of HDACs (Figure 3). Treatment of HCT 116 cells with compound **51** gave rise to elevated and dose-dependent levels of acetylated histone H4 and $p21^{WAF1/CIP1}$.

Inhibitory Mechanism Study. Since the results of cancer cell growth inhibition and Western blot analysis have suggested that thiols generated from *S*-acyl prodrugs by enzymatic hydrolysis within the cell inhibit intracellular HDACs, we next studied the mechanism by which thiols inhibit HDACs in greater detail. Although the sulfhydryl group of thiol derivatives was designed as a ZBG, it is possible that thiols inhibit HDACs by forming a covalent disulfide bond with cysteine residues on these enzymes. We examined this possibility using a double reciprocal plot of 1/V versus 1/[substrate] at varying concentrations of inhibitor **7** (Figure 4), and the data from this study established that thiol **7** engages in competitive inhibition versus acetylated lysine substrate, with an inhibition constant (K_i) of 0.11 μM. Since cysteine is not a component in the construction of the active site of HDACs, the sulfhydryl group of **7** likely interacts with the zinc in the active site.

Binding Mode Study. Since thiol **7** proved to be a competitive inhibitor and to act within the active center of HDACs, we studied its binding mode within this site. The low energy conformations of **7** and SAHA were calculated when docked in the model based on the crystal structure of HDAC8 (PDB code 1T64, 1T67, 1T69, and 1VKG) using Macromodel 8.1 software.[25] The anilide group and alkyl chain of **7** and SAHA were essentially superimposed in the binding pocket, and the binding mode of **7** was found to be similar to that of SAHA (Figure 5, left). An inspection of the HDAC8/**7** complex shows that the sulfur atom of **7** was located 2.35 Å from the zinc ion, 2.24 Å from the OH group of Tyr 306, and 2.66 Å from a water molecule which forms a hydrogen bond with the imidazole group of His142 (Figure 5, right). This suggests that thiols strongly inhibit HDACs by interacting directly with zinc ion, Tyr 306, and His 142 via a water molecule.

Conclusion

We have designed and prepared a series of SAHA-based compounds as (i) hydroxamic acid mimics by structure-based drug design (compounds **4**–**6**), (ii) thiol-based analogues (compounds **7**–**9**), (iii) transition-state analogues (compounds **10** and **11**), (iv) heteroatom-containing substrate analogues by mechanism-based drug design (compounds **12**–**15**), and (v) irreversible inhibition-oriented compounds (compounds **16**–**18**), and evaluated their inhibitory effect on HDACs. In this series, thiol **7** and mercaptoacetamide **14** were found to be much more potent HDAC inhibitors than previously reported non-hydroxamates, and as potent as α-ketoamide **2** and SAHA. At present, thiol is one of the most active ZBG among small-molecule HDAC inhibitors. Optimization of thiol derivatives led to the identification of inhibitors more effective than SAHA (compounds **26**, **30**, **34**, and **35**). We have also identified a potent cancer cell growth inhibitor, compound **51**, by the prodrug formation of thiol-based HDAC inhibitors. Thiol **7** exhibits strong competitive inhibition of an acetylated lysine substrate, and molecular modeling suggests that the thiol interacts with zinc, Tyr 306, and His 142 (HDAC8 numbering) in the active site.

In conclusion, we have identified several new lead structures including thiol, from which more potent HDAC inhibitors can be developed. As far as we could determine, this is the first systematic study of ZBGs for HDAC inhibitors. We believe that the findings of this study should be of value in future studies for the development of ideal anticancer drugs and tools for biological research such as HDAC isozyme-selective inhibitors.

Experimental Section

Chemistry. Melting points were determined using a Yanagimoto micro melting point apparatus or a Büchi 545 melting point apparatus and were left uncorrected. Proton nuclear magnetic resonance spectra (^{1}H NMR) were recorded on a JEOL JNM-LA400 or JEOL JNM-LA500 spectrometer in solvent as indicated. Chemical shifts (δ) are reported in parts per million relative to the internal standard tetramethylsilane. Elemental analysis was performed with a Yanaco CHN CORDER NT-5 analyzer, and all values were within ±0.4% of the calculated values. High-resolution mass spectra (HRMS) were recorded on a JEOL JMS−SX102A mass spectrometer. GC-MS analyses were performed on a Shimadzu GCMS-QP2010. Reagents and solvents were purchased from Aldrich, Tokyo Kasei Kogyo, Wako Pure Chemical Industries, and Kanto Kagaku and used without purification. Flash column chromatography was performed using silica gel 60 (particle size 0.046−0.063 mm) supplied by Merck.

6-(3-Hydroxyureido)hexanoic Acid Phenylamide (4). Step 1: Preparation of 6-Phenylcarbamoylhexanoic Acid (57). A mixture of aniline (5.80 g, 62.3 mmol) and pimeric acid (**56**, 10.0 g, 62.4 mmol) was stirred at 180 °C for 1 h. After cooling, the mixture was diluted with AcOEt-THF and the slurry was filtered. The filtrate was washed with saturated aqueous $NaHCO_3$, and the aqueous layer was acidified with concentrated HCl. The precipitated crystals were collected by filtration to give 7.11 g (49%) of **57** as a white solid: ^{1}H NMR (DMSO-d_6, 400 MHz, δ; ppm) 11.97 (1H, broad s), 9.83 (1H, s), 7.58 (2H, d, J = 7.8 Hz), 7.27 (2H, t, J = 7.9 Hz), 7.01 (1H, t, J = 7.4 Hz), 2.67 (2H, t, J = 7.4 Hz), 2.21 (2H, t, J = 7.3 Hz), 1.62−1.49 (4H, m), 1.34−1.27 (2H, m).

Steps 2 and 3: Preparation of 6-(3-Hydroxyureido)-hexanoic Acid Phenylamide (4). To a suspension of **57** (958 mg, 4.07 mmol) obtained above and triethylamine (744 mg, 7.35 mmol) in toluene (10 mL) was added diphenylphosphoryl azide (1.75 g, 6.34 mmol), and the mixture was heated at reflux temperature for 1h. Next, *O*-(2-tetrahydropyranyl)hydroxylamine (380 mg, 3.11 mmol) was added, and the reaction mixture was stirred at reflux temperature for 18h. It was then concentrated in vacuo, and the residue was dissolved in AcOEt. The AcOEt solution was washed with water, saturated aqueous $NaHCO_3$, and brine and was dried over Na_2SO_4. Filtration and concentration in vacuo and purification by silica gel flash chromatography (*n*-hexane/AcOEt = 1/2) gave 988 mg (69%) of the *O*-(2-tetrahydropyranyl)hydroxyurea as a white solid: ^{1}H NMR ($CDCl_3$, 500 MHz, δ; ppm) 7.53 (2H, d, J = 7.9 Hz), 7.32 (2H, t, J = 7.8 Hz), 7.26 (1H, broad s), 7.10 (1H, t, J = 7 Hz), 7.05 (1H, broad s), 6.06 (1H, broad s), 4.75 (1H, d, J = 3.6 Hz), 3.93 (1H, m), 3.57 (1H, m), 3.33−3.26 (2H, m), 2.38 (2H, t, J = 7.5 Hz), 1.82−1.77 (4H, m), 1.61−1.55 (6H, m), 1.44 (2H, quintet, J = 7.3 Hz).

To a solution of the *O*-(2-tetrahydropyranyl)hydroxyurea (185 mg, 0.53 mmol) obtained above in MeOH (2 mL) was added 4-toluenesulfonic acid monohydrate (15 mg, 0.079 mmol). The solution was stirred overnight at room temperature, and the precipitated crystals were collected by filtration to give 46 mg (32%) of **4** as a white solid. The solid was recrystallized from MeOH–AcOEt and collected by filtration to give 34 mg of **4** as a colorless crystal: mp 148–149 °C; ^{1}H NMR (DMSO-d_6, 500 MHz, δ; ppm) 9.93 (1H, s), 8.58 (1H, s), 8.29 (1H, s), 7.65 (2H, d, J = 8 Hz), 7.35 (2H, t, J = 7.9 Hz), 7.08 (1H, t, J = 7.3 Hz), 6.75 (1H, t, J = 6 Hz), 3.10 (2H, q, J = 6.7 Hz), 2.36 (2H, t, J = 7.5 Hz), 1.65 (2H, quintet, J = 7.5 Hz), 1.50 (2H, quintet, J = 7.2 Hz), 1.34 (2H, quintet, J = 7.6 Hz); Anal. ($C_{13}H_{19}N_3O_3$) C, H, N.

6-(3-Aminoureido)hexanoic Acid Phenylamide (5). Compound **5** was prepared from **57** obtained above by using the procedure described for **4** (step 2) in 52% yield. In this case, hydrazine monohydrate was used instead of *O*-(2-tetrahydropyranyl)hydroxylamine: mp 146–147 °C; ^{1}H NMR (DMSO-d_6, 400 MHz, δ; ppm) 9.83 (1H, s), 7.58 (2H, d, J = 7.8 Hz), 7.27 (2H, t, J = 7.9 Hz), 7.01 (1H, t, J = 7.3 Hz), 6.83 (1H, broad s), 6.28 (1H, broad s), 4.03 (2H, broad s), 3.01 (2H, q, J = 6.7 Hz), 2.29 (2H, t, J = 7.4 Hz), 1.60–1.57 (2H, m), 1.40–1.38 (2H, m), 1.32–1.28 (2H, m); MS (EI) *m/z*: 264 (M^+); Anal. ($C_{13}H_{20}N_4O_2$) C, H, N.

6-Methanesulfonylaminohexanoic Acid Phenylamide (10). Steps 1 and 2: Preparation of 6-Aminohexanoic Acid Phenylamide (58). To a suspension of **57** (1.11 g, 4.73 mmol) obtained above and triethylamine (699 mg, 6.90 mmol) in benzene (3 mL) was added diphenylphosphoryl azide (1.83 g, 6.64 mmol), and the mixture was heated at reflux temperature for 1 h. Next, benzyl alcohol (1.20 mL, 11.6 mmol) was added, and the reaction mixture was stirred at reflux temperature for 24 h. It was then concentrated in vacuo and the residue was dissolved in AcOEt. The AcOEt solution was washed with 0.4 N aqueous HCl, water, saturated aqueous $NaHCO_3$, and brine and was dried over Na_2SO_4. Filtration and concentration in vacuo and purification by recrystallization from $CHCl_3$–*n*-hexane gave 1.01 g (63%) of (6-phenylcarbamoylpentyl)carbamic acid benzyl ester as a colorless needle: ^{1}H NMR (DMSO-d_6, 400 MHz, δ; ppm) 9.81 (1H, s), 7.57 (2H, d, J = 7.8 Hz), 7.37–7.22 (8H, m), 7.00 (1H, t, J = 7.4 Hz), 4.99 (2H, s), 2.99 (2H, q, J = 6.5 Hz), 2.28 (2H, t, J = 7.4 Hz), 1.58 (2H, quintet, J = 7.6 Hz), 1.43 (2H, quintet, J = 7.1 Hz), 1.32 (2H, quintet, J = 7.8 Hz); MS (EI) *m/z*: 340 (M^+).

A solution of (6-phenylcarbamoylpentyl)carbamic acid benzyl ester (1.00 g, 2.95 mmol) obtained above in MeOH (50 mL) was stirred under H_2 (atmospheric pressure) in the presence of 5% Pd/C (106 mg) at room temperature for 7 h. The catalyst was removed by filtration through Celite, and the filtrate was concentrated in vacuo. The residue was purified by silica gel flash chromatography ($CHCl_3$/MeOH/*i*PrNH$_2$ = 19/1/1) to give 584 mg (96%) of **58** as a white solid: ^{1}H NMR (DMSO-d_6, 400 MHz, δ; ppm) 9.83 (1H, s), 7.58 (2H, d, J = 7.6 Hz), 7.27 (2H, t, J = 7.9 Hz), 7.01 (1H, t, J = 7.3 Hz), 2.55 (2H, m), 2.29 (2H, t, J = 7.4 Hz), 1.59 (2H, quintet, J = 7.4 Hz), 1.37–1.30 (4H, m).

Step 3: Preparation of 6-Methanesulfonylaminohexanoic Acid Phenylamide (10). To a solution of **58** (500 mg, 2.06 mmol) obtained above in pyridine (5 mL) was added methanesulfonyl chloride (160 μL, 2.07 mmol) dropwise with cooling in an ice–water bath. The solution was stirred for 30 min at room temperature. The mixture was concentrated and diluted with AcOEt. The solution was washed with 2 N aqueous HCl, water, and brine and was dried over Na_2SO_4. Filtration and concentration in vacuo and purification by silica gel flash chromatography (*n*-hexane/AcOEt = 1/3) gave 418 mg (71%) of **10** as a crude solid. The solid was recrystallized from AcOEt to give **10** (214 mg) as colorless crystals: mp 136–137 °C; ^{1}H NMR (DMSO-d_6, 500 MHz, δ; ppm) 9.85 (1H, s), 7.58 (2H, d, J = 7.7 Hz), 7.28 (2H, t, J = 7.4 Hz), 7.01 (1H, t, J = 7.4 Hz), 6.93 (1H, t, J = 6.5 Hz), 2.92 (2H, q, J = 6.5 Hz), 2.87 (3H, s), 2.30 (2H, t, J = 7.6 Hz), 1.59 (2H, quintet, J = 7.6 Hz), 1.59 (2H, quintet, J = 7.6 Hz), 1.48 (2H, quintet, J = 7.4 Hz), 1.33 (2H, quintet, J = 7.4 Hz); MS (EI) *m/z*: 284 (M^-); Anal. ($C_{13}H_{20}N_2O_3S$) C, H, N.

6-(2-Hydroxyacetylamino)hexanoic Acid Phenylamide (13). To a solution of **58** (198 mg, 0.96 mmol) and glycolic acid (81 mg, 1.07 mmol) in DMF (6 mL) were added 1-ethyl-3-(3-dimethylaminopropyl)carbodiimide hydrochloride (254 mg, 1.32 mmol) and 1-hydroxy-1*H*-benzotriazole monohydrate (244 mg, 1.59 mmol), and the mixture was stirred overnight at room temperature. The reaction mixture was poured into water and extracted with AcOEt. The AcOEt layer was separated, washed with saturated aqueous $NaHCO_3$ and brine, and dried over Na_2SO_4. Filtration and concentration in vacuo gave 251 mg (99%) of **13** as a crude solid. The solid was recrystallized from AcOEt to give 155 mg of **13** as a colorless crystal: mp 109–113 °C; ^{1}H NMR (DMSO-d_6, 500 MHz, δ; ppm) 9.92 (1H, s), 7.79 (1H, broad s), 7.65 (2H, d, J = 7.6 Hz), 7.35 (2H, t, J = 7.9 Hz), 7.08 (1H, t, J = 7.3 Hz), 5.51 (1H, t, J = 5.8 Hz), 3.84 (2H, d, J = 5.8 Hz), 3.16 (2H, q, J = 6.8 Hz), 2.36 (2H, t, J = 7.5 Hz), 1.65 (2H, quintet, J = 7.5 Hz), 1.51 (2H, quintet, J = 7.3 Hz), 1.35 (2H, quintet, J = 7.9 Hz); MS (EI) *m/z*: 264 (M^+); Anal. ($C_{14}H_{20}N_2O_3$) C, H, N.

6-(2-Aminoacetylamino)hexanoic Acid Phenylamide Trifluoroacetic Acid Salt (12·TFA). Step 1: Preparation of [(5-Phenylcarbamoylpentylcarbamoyl)methyl]carbamic Acid *tert*-Butyl Ester. This compound was prepared from **58** and *N*-(*tert*-butoxycarbonyl)glycine using the procedure described for **13** in 70% yield: ^{1}H NMR ($CDCl_3$, 400 MHz, δ; ppm) 7.53 (2H, d, J = 7.8 Hz), 7.34 (2H, t, J = 7.6 Hz), 7.10 (1H, t, J = 7.6 Hz), 6.14 (1H, broad s), 5.07 (1H, broad s), 3.75 (2H, d, J = 6 Hz), 3.30 (2H, q, J = 6.5 Hz), 2.37 (2H, t, J = 7.4 Hz), 1.76 (2H, quintet, J = 7.4 Hz), 1.58–1.26 (13H, m).

Step 2: Preparation of 6-(2-Aminoacetylamino)hexanoic Acid Phenylamide Trifluoroacetic Acid Salt (12·TFA). To a solution of [(5-phenylcarbamoylpentylcarbamoyl)-methyl]carbamic acid *tert*-butyl ester (147 mg, 0.40 mmol) obtained above in $CHCl_3$ (4 mL) was added trifluoroacetic acid (1 mL), and the mixture was stirred overnight at room temperature. The reaction mixture was concentrated in vacuo, and the residue was triturated in diethyl ether to give 131 mg (84%) of **12**·TFA as a white solid. The solid was recrystallized from AcOEt–MeOH to give 120 mg of **12**·TFA as colorless crystals: mp 149–151 °C; ^{1}H NMR (DMSO-d_6, 500 MHz, δ; ppm) 10.00 (1H, s), 8.43 (1H, t, J = 5.2 Hz), 8.10 (3H, broad s), 7.71 (2H, d, J = 8.2 Hz), 7.41 (2H, t, J = 7.9 Hz), 7.14 (1H, t, J = 7.3 Hz), 3.25 (2H, q, J = 6.4 Hz), 2.43 (2H, t, J = 7.3 Hz), 1.72 (2H, quintet, J = 7.5 Hz), 1.58 (2H, quintet, J = 7.2 Hz), 1.44 (2H, quintet, J = 7.5 Hz); Anal. ($C_{14}H_{21}N_3O_2$·TFA·1/10H_2O) C, H, N.

6-(2-Bromoacetylamino)hexanoic Acid Phenylamide (18). To a solution of **58** (70 mg, 0.340 mmol) and triethylamine (0.40 mL, 2.88 mmol) in THF (2 mL) was added a solution of bromoacetyl bromide (319 mg, 1.58 mmol) in THF (1 mL) dropwise with cooling in an ice–water bath. The mixture was stirred at room temperature for 30 min. The reaction mixture was diluted with $CHCl_3$, washed with aqueous saturated $NaHCO_3$, water, and brine, and dried over Na_2SO_4. Filtration and concentration in vacuo and purification by silica gel flash chromatography ($CHCl_3$/MeOH = 150/1) gave 25 mg (23%) of **18** as a white solid: ^{1}H NMR ($CDCl_3$, 400 MHz, δ; ppm) 7.52 (2H, d, J = 8.1 Hz), 7.32 (2H, t, J = 7.9 Hz), 7.19 (1H, broad s), 7.10 (1H, t, J = 7.6 Hz), 6.56 (1H, broad s), 3.87 (2H, s), 3.32 (2H, q, J = 6.6 Hz), 2.38 (2H, t, J = 7.3 Hz), 1.80–1.76 (2H, m), 1.63–1.59 (2H, m), 1.46–1.44 (2H, m); MS (EI) *m/z*: 326 (M^+); Anal. ($C_{14}H_{19}BrN_2O_2$) C, H, N.

Thioacetic acid *S*-[(6-Phenylcarbamoylpentylcarbamoyl)methyl] Ester (15). To a suspension of **18** (187 mg, 0.57 mmol) obtained above in EtOH (2 mL) was added potassium thioacetate (236 mg, 2.07 mmol), and the mixture was stirred at room temperature for 16 h. The reaction mixture was diluted with AcOEt and THF, washed with water and brine, and dried over Na_2SO_4. Filtration and concentration in vacuo and purification by silica gel flash chromatography (*n*-hexane/AcOEt = 1/1) gave 163 mg (89%) of **15** as a white solid. The solid was recrystallized from *n*-hexane–AcOEt to give 48 mg